The Petrology and Geochemistry of Coastal Dikes from São Paulo State, Brazil: Implications for Variable Lithospheric Contributions to Alkaline Magmas from the Western Margin of the South Atlantic

GIANNA M. GARDA[1], JOHANN H. D. SCHORSCHER[2], SONIA ESPERANÇA[3] and RICHARD W. CARLSON[4]

[1]Instituto Geológico, Secretaria de Estado do Meio Ambiente, São Paulo, SP, Brazil
[2]Instituto de Geociências, Universidade de São Paulo, São Paulo, SP, Brazil
[3]Institute of Earth and Planetary Sciences, Monash University, Australia
[4]Department of Terrestrial Magnetism, Carnegie Institution of Washington, USA

ABSTRACT

Cretaceous mafic igneous activity in Southern Brazil is characterized by a variety of rock types ranging from tholeiitic basalts to a suite of unusual alkaline compositions. Along the coastline between São Sebastião and Ubatuba cities (São Paulo State, Brazil) the Archean and Proterozoic rocks of the Costeiro Complex are crosscut not only by basaltic dikes but also by camptonites-monchiquites, biotite lamprophyres, including a melilite-bearing variety (alnöite), and picritic lamprophyres.

The basaltic dikes show phenocrysts of plagioclase (labradorite/andesine), pyroxene (augite/pigeonite) and iron ores in a very fine to fine-grained groundmass of similar mineral composition. When coarser grained, granophyric quartz and alkali feldspar intergrowths may be present. In contrast, the lamprophyric dikes present abundant megacrysts of pseudomorphosed olivine (± chromite inclusions) and pyroxene. The groundmass is composed by titaniferous augite, kaersutite, Mg-rich biotite, feldspars (plagioclase and K-feldspar), iron ores, analcime (in monchiquites) and devitrified glass. Carbonates are fairly common.

The basaltic dikes have low Mg# (*ca.* 30) as opposed to the lamprophyres (Mg# = 57-71; *ca.* 80 for picritic lamprophyres). SiO_2, Al_2O_3, Na_2O and K_2O contents are higher and FeO_t, MgO and CaO are lower in the basaltic dikes when compared to the lamprophyres. For the lamprophyres, $SiO_2 < 47\%$, $Al_2O_3 < 12\%$ and $MgO > 10\%$. Furthermore, the picritic lamprophyres have the lowest TiO_2, P_2O_5, Al_2O_5, FeO_t, Na_2O and K_2O contents.

The high field strength elements in the basaltic dikes define small negative anomalies (*e.g.* Nb and Ta) as opposed to positive anomalies in the picritic lamprophyres. Incompatible element concentrations are higher in the basaltic dikes and lower in the picritic lamprophyres, when both are compared to the monchiquites-camptonites and biotite lamprophyres.

Distinct mantle sources for the coastal dikes are indicated by preliminary Sr, Nd and Pb isotopic data. The basaltic dikes have $\varepsilon_{Nd}(i)$ of *ca.* –5 and initial $^{87}Sr/^{86}Sr$ of 0.706 to 0.707, falling in the ranges found in the literature for the low and high-Ti Paraná basalts. In contrast, samples from the lamprophyric types show

Correspondence to: Gianna M. Garda
Instituto Geológico, Av. Miguel Stéfano 3900,
CEP 04301-903 São Paulo, SP, Brazil

$\varepsilon_{Nd}(i)$ between +1 and +2 and initial $^{87}Sr/^{86}Sr$ around 0.705 which are distinctly different from values found for any Paraná basalts and may indicate a deeper mantle source with greater proportions of asthenospheric-derived melts.

The alnöite is highly enriched in radiogenic Pb ($^{206}Pb/^{204}Pb$ = 19.94), whereas $^{206}Pb/^{204}Pb$ data for the other dike-rocks fall between 18.21 and 18.71. All samples lie well above the Northern Hemisphere Reference Line on $^{207}Pb/^{204}Pb$ *vs.* $^{206}Pb/^{204}Pb$ plot, where, again, the basaltic dikes fall in the field of the Paraná basalts.

The geochemical data support a distinct input of mantle components in the generation of the basaltic and lamprophyric dikes. Whereas the former is related to the Paraná Basin magmatism, the latter may be associated with an alkaline magmatic event intermediate in age between the intrusion of the basaltic dikes (130 Ma) and that of the nepheline-syenite complex of São Sebastião Island (*ca.* 80 Ma), as indicated by $^{87}Sr/^{86}Sr$ isochrons.

Key words: mafic dikes, alkaline lamprophyres, alnöite, Mesozoic volcanism.

INTRODUCTION

The Mesozoic magmatism in Southern Brazil is represented by the basalts of the Serra Geral Formation, the dike swarms of the Ponta Grossa Arch, the mafic dikes along the coast between São Paulo and Rio de Janeiro and several alkaline complexes that lie along tectonic features associated with the evolution of the Paraná Basin (Almeida, 1983).

The mafic dikes which are object of this study occur along the coast between São Sebastião and Ubatuba cities (São Paulo State) and crosscut Archean and Proterozoic rocks of the Costeiro Complex. They can also be found in São Sebastião, Mar Virado and Anchieta Islands (Fig. 1).

The first detailed mapping, petrographic description and classification of the basic dikes of the Ubatuba region and Mar Virado and Anchieta islands was published by Damasceno (1966). Several occurrences were also mapped in regional projects (*e.g.* Freitas, 1976; Silva *et al.*, 1977). Chieregati *et al.* (1982) and Chiodi Filho *et al.* (1983) described diabases, diorites, porphyry diorites and latites in the region represented in the Natividade da Serra and Caraguatatuba 1:50,000 sheets (see also DAEE-UNESP, 1989). Comin-Chiaramonti *et al.* (1983) presented chemical analyses of samples collected in the Peruíbe region and along the BR-101 Highway, from Ubatuba to Angra dos Reis, that were later compared to the dike swarm of the Ponta Grossa Arch by Piccirillo *et al.* (1988a).

A few papers emphasized mineralogical an petrochemical aspects of particular dike occu rences, such as the Toninhas dike (Gomes, 197 Gomes, 1974; Gomes & Ruberti, 1979; Gomes Berenholc, 1980), the traverse form Ponta d Baleeiro, near São Sebastião City, to Ilha Bela, Sã Sebastião Island (Coutinho *et al.*, 1991) and th mafic and ultramafic dikes of Praia Vermelha d Sul (Garda *et al.*, 1992). Coutinho & Ens (199 presented the first results of their petrographic an petrogenetic study of the dikes that occur betwee Itanhaém and São Sebastião cities.

Freitas (1947) studied the geology of the Sã Sebastião Island in great detail, including the dik that crosscut the Western margin of the island ar the Bonete Beach. These were later analysed ar presented in the geochronological study of Bellie *et al.* (1990).

FIELD CHARACTERISTICS

As pointed out by Damasceno (1966) a stri ing feature is the predominant N55E direction the dikes, which coincides with the main region lineaments of the country rock and Serra do M escarpment. Along the coast, the dikes are qui fresh and form small, irregularly distribut swarms. The dikes can be a few centimeters to se eral meters thick and may show branching. Wh eroded, blocks of different sizes may be found ne to or filling the emplacement fractures. Howev dike rims may still be preserved, welded to t country rock.

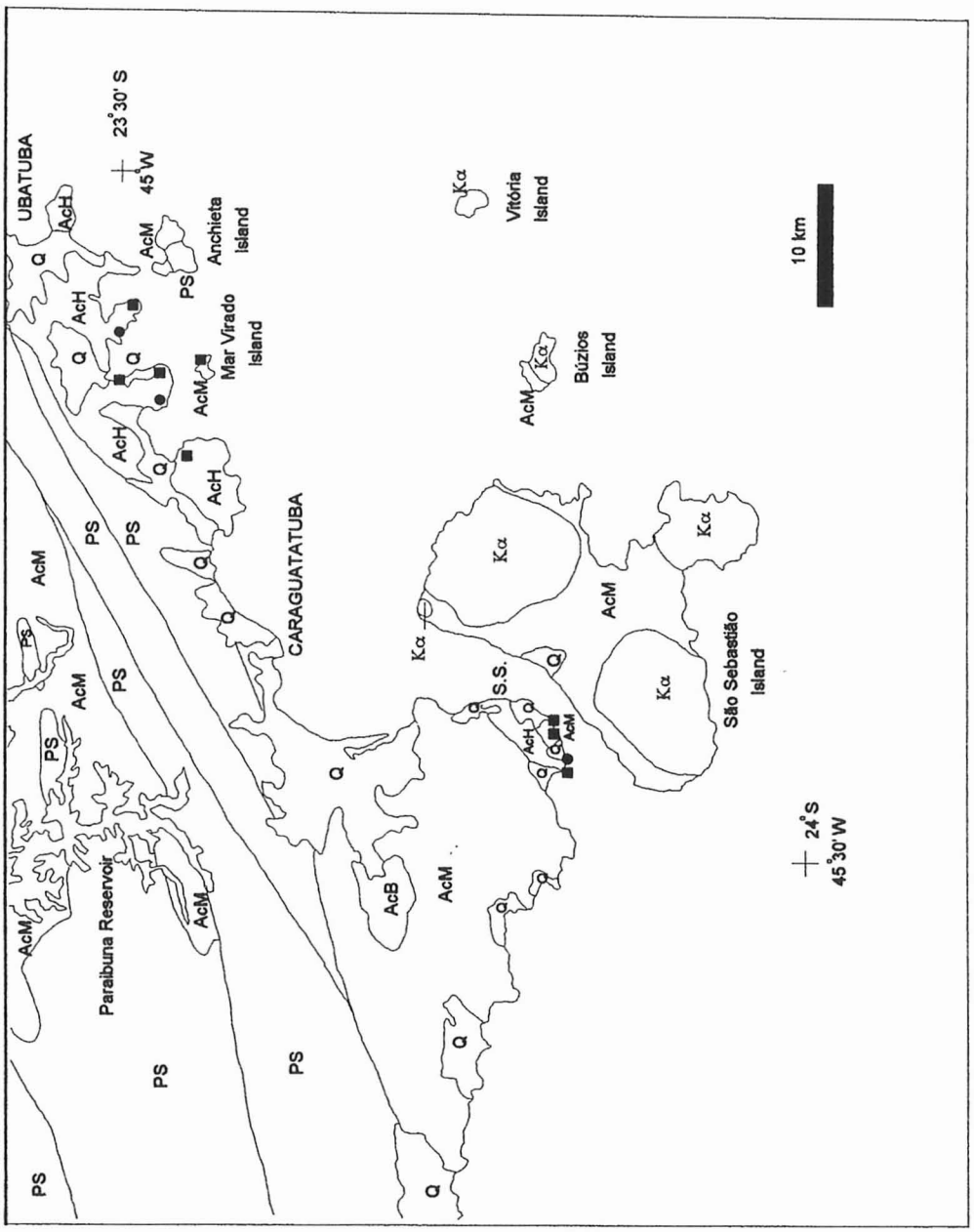

Fig. 1 — Distribution of mafic dikes along the coast between São Sebastião (S.S.) and Ubatuba cities, São Sebastião, Mar Virado and Anchieta islands (Almeida *et al.*, 1981, mod.). Archean rocks of the Costeiro Complex: AcH = granulites; AcM = migmatitic rocks; AcB = metamorphosed basic rocks. Upper Proterozoic: PS = granitic rocks. Mesozoic: ● = dikes of basaltic composition (BAS); ■ = dikes of lamprophyric affinity (LAMP); Kα = alkaline igneous rocks. Q = Quaternary deposits.

The dikes can be classified in the field as belonging to a basaltic (BAS) and a lamprophyric (LAMP) groups.

The BAS group include aphanitic (also glassy), aphyric and porphyritic types, the groundmass being fine to very fine or glassy in the latter. Thicker dikes may present differentiated, coarser cores and glassy or chilled rims. The predominant color is dark gray to black, gaining a rusty-brownish tint upon weathering.

Some of the rock types which belong to the LAMP group can be recognized in the field by the presence of abundant olivine and pyroxene megacrysts, which, when weathered, leave cavities in the rock. The groundmass is generally aphanitic and dark gray to black.

PETROGRAPHY

In the BAS group, phenocrysts and microphenocrysts of plagioclase, augitic (and to a lesser extent, pigeonitic) pyroxene and iron ores are present in a very fine to fine groundmass where plagioclase and pyroxene occur in similar proportions and where opaque minerals may be skeletal. In the coarser portions of the thicker dikes feldspar may predominate and intergrowths of alkali feldspar and quartz also occur. Biotite and apatite are (un)common accessory phases in the evolved centers. The common alteration minerals are sericite and chlorite. Very fine veins filled with quartz, carbonate and/or chlorite may occur, as well as small country rock xenoliths.

The LAMP group can be further subdivided into alkaline-camptonites and monchiquites, and ultramafic-alnöite, lamprophyres. Camptonites present abundant megacrysts of pseudomorphosed olivine and pyroxene, sometimes arranged in a glomeroporphyritic texture. The groundmass is mainly composed of titaniferous augite, followed by kaersutite, biotite, plagioclase, iron ores and interstitial matter of very low birefringence, that may include chlorite. Carbonate occurs in the groundmass. Regarding the presence of carbonates, Rock (1986) comments that although distinction should be made between primary and secondary carbonates, his classification for ultramafic lamprophyres is based on present mineralogy and total carbonates may be used and computed in color index estimations.

Monchiquites present analcime and glass in addition to the mineralogy of the camptonites. The glass is colorless or transparent brown, rich in microlites, such as in Hunter & Rosenbusch's (1890, *in*: Rock, 1979) description of the type-monchiquite. Monchiquites and camptonites also present variable amounts of up to 1mm-large globular structures (occelli) filled with carbonate (in the camptonites) and carbonate + analcime (in the case of monchiquites).

Biotite may supersede kaersutite in the monchiquites, and occasionally occurs as phenocrysts. A biotite-rich monchiquite is termed ouachitite. However, Rock (1986) considers that even the type-rock has mineral and bulk composition tending to ultramafic rather than to alkaline lamprophyre and suggests the term "ouachitite" be applied to an ultramafic lamprophyre with essential feldspathoids and carbonates, with or without melilite. It was, then, decided to name the biotite-rich lamprophyres from this work biotite lamprophyres.

A sole example of an ultramafic lamprophyre is the alnöite found in Caçandoca Beach, which was included in the biotite lamprophyre subgroup. Melilite is recognized by its anomalous blue interference color and peg structure. Together with Ca-rich pyroxene, they form the bulk of the rock. Zoned biotite and Mg-rich chromite are the other rock-forming minerals. A possible melanitic, non-isotropic garnet was also found. Silicates (feldspar and probably feldspathoids) fill some of the occelli. According to Rock (1986), ultramafic lamprophyres are intimately associated with carbonatites in continental rifts, either in lamprophyre-carbonatite dike swarms, nepheline-carbonatite volcanoes, intrusive carbonatite (-ijolite-syenite, etc.) complexes, or as isolated dike swarms or in a concentration of plugs in both continental and oceanic settings. Although direct evidences of carbonatite bodies were not found in the region, the presence, mainly in the biotite lamprophyres, of carbonate fragments, sometimes showing reaction rims and corrosion textures, may indicate a genetic associa-

tion with carbonatitic liquids. Dikes from the coast of Itanhaém (South coast of São Paulo State) were described as of carbonatitic composition (Melcher & Coutinho, personal communication, *in*: Sonoki & Garda, 1988; Coutinho & Ens, 1992).

A megacryst-rich variety of LAMP, with cumulate texture, was also found in the area and is here named picritic lamprophyre. Olivine is fresh and not rarely associated with pyroxene. Chromite is not only included in olivine, but may also be found in the matrix. The groundmass is aphanitic, very fine to fine, dominated by pyroxene. Kaersutite and biotite are almost absent.

MINERAL CHEMISTRY

Mineral analyses were carried out at the Centre for Microscopy and Microanalysis of the University of Western Australia (SEM + EDS, JEOL 6400) and at the Centre for Petrology and Lithospheric Studies of Macquarie University, Australia (WDS, CAMECA SX 50). Some of the results are briefly presented. More detailed discussions of the mineral analyses can be found in Garda (1995).

The compositions of the feldspars in BAS dikes vary in the range $An_{50}Ab_{44}Or_6$-$An_{43}Ab_{50}Or_7$, corresponding to labradorite/andesine plagioclase. On the other hand, granophyric intergrowths, crystallized in the more evolved centers of the thicker BAS dykes, are formed by quartz and alkali feldspar ($Ab_{29}Or_{71}$ and $Ab_{59}Or_{41}$).

BAS pyroxenes are poorer in CaO ($Wo_{41}En_{41}Fs_{18}$-$Wo_{30}En_{34}Fs_{36}$) when compared to LAMP.

A brown amphibole also appears in BAS. The ranges in composition are: SiO_2: 43-46%, TiO_2: 1.6-1.0%, Al_2O_3: 4.7-6.4%, FeO: 24-25%, MnO: 0.3-0.4%, MgO: 7.2-8.4%, CaO: 9.7-10.4%, Na_2O: 1.5-2.0%, K_2O: 0.6-1.1%, NiO: 0-0.07%, F: 1.0-1.4% and Cl: 0.19-0.46%, which correspond to a iron-hornblende.

Less calcic feldspar compositions are found in LAMP ($An_{35}Ab_{57}Or_8$). On the other hand, their pyroxene compositions cluster around $Wo_{52}En_{40}Fs_8$, being the extreme case the alnöite, with $Wo_{61}En_{33}Fs_6$. These compositions fall in the Quadrilateral field of the Ca-Fe-Mg pyroxenes (Morimoto, 1988). However, such diagram does not emphasize their TiO_2 content, which can reach 7.9%.

LAMP may present zoned biotites, with phlogopitic cores (Mg# between 73 and 79) and biotitic rims (Mg# between 5 and 25), or vice-versa. When not zoned, phlogopite compositions predominate (Mg# between 78 and 81).

Kaersutite (in camptonites and monchiquites) analyses are typically: SiO_2: 36.5-39.7%, TiO_2: 4.26-6.64%, Al_2O_3: 13.29-15.17%, FeO: 11.06-15.16%, MnO: 0-0.27%, MgO: 8.82-11.48%, CaO: 11.97-12.43%, Na_2O: 1.55-1.99% and K_2O: 1.32-1.62%. Some compositions are poorer in Ti and the mineral is classified as a titanian ferroan pargasite (Leake, 1978).

Rock (1991) states that analcime analyses generally do not reach the ideal formula $NaAlSi_2O_6.H_2O$ and that FeO impurities are common. Furthermore, the mineral can dehydrate and loose Na under the electron beam. Here, analcime analyses close very badly around 88%.

The alnöite melilite compositions are: SiO_2: 43%, Al_2O_3: 6%, FeO: 3%, MgO: 8,5%, CaO: 37,5% and Na_2O: 2%, which correspond to a solid solution of 60% äkermanite, 22% Na-melilite, 10% $Ca_2FeSi_2O_7$ and 7% gehlenite. These compositions are in agreement with the proportions of 1/3 Na-melilite and 2/3 äkermanite that are found in typical alnöites (Rock, 1986) and are characterized by a deficiency in the gehlenite end-member that is commonly observed in volcanic-subvolcanic rocks (Edgar, 1984).

Apatites, although abundant in LAMP, are very fine, making the analyses difficult. There are WDS indications that these apatites are fluorine-rich.

Although carbonates are not stable under the electron beam, the analyses of carbonate fragments found in biotite lamprophyres ($FeCO_3$: 4-67%, $MgCO_3$: 20-82%, $CaCO_3$: 1-59% and $MnCO_3$: 0-1%) differ from the compositions of the carbonates (calcite) that fill globular structures (occelli) or appear in the groundmass. Rock (1986) suggests four possible origins for Mg-rich carbonates in ul-

tramafic lamprophyres: primary crystallization, carbonation of primary silicates, dolomitization of primary calcite and dolomitization of secondary calcite. However, under the microscope, the textural evidence shows that the high Mg-carbonate fragments are xenoliths from a carbonatite body, whereas the occelli and groundmass carbonates are probably derived from the crystallization of the magma.

The fresh cores of partially pseudomorphosed olivine megacrysts are forsterite-rich (85-87%) and are found in the picritic lamprophyres. According to Rock (1979), such olivine compositions are typical of alkaline picrites. He interprets breccia clasts from Serra de Monchique (Portugal) as xenoliths of a cumulative picritic layer which formed in the early stages of the evolution of the Monchique Complex.

Chromites of the alnöite present cores with average compositions of Cr# = 100 Cr/(Cr+Al) = 22, Fe# = 100 Fe/(Fe+Mg) = 30 and Ti# = 100 Ti/(Ti+Al+Cr) = 1, as opposed to reaction rims for which Cr# = 1, Fe# = 60 and Ti# = 25. Camptonite chromites present the average composition: $Ulvo_7Sp_{42}Cr_{37}Mt_{14}$ and those of the picritic lamprophyres: $Ulvo_1Sp_{56}Cr_{36}Mt_7$.

Exsolutions of titanomagnetite in ilmenite were observed in the EDS images. Analyses were generally not good (totals < 100%) and the calculation of Fe^{3+} according to Droop (1987) yields high values for the hematite molecule (oxidation effect?). Only a small percentage of the compositions present $TiO_2 > 41\%$. As pointed out by Rock (1986), fairly high Mg and Mn may be diagnostic of ultramafic lamprophyre ilmenites. In the alnöite, the ilmenites are more picritic (MgO = 7%) and less MnO-rich (1.3%) than those in the other rock types (MgO = 5.5% and MnO = 2-3%).

MAJOR ELEMENTS

The major elements, analysed by X-ray fluorescence at the Geochemistry Laboratory of the Geology and Paleontology Institute of the Hamburg University (Germany), are listed in Table I. Normative minerals were calculated using the program NEWPET (Clarke, 1992), assuming 85% of all iron as FeO, CO_2 to calculate calcite, Cr_2O_3 for chromite and S for pyrite.

Not always BAS dikes are quartz-normative, although their Mg# values are comparatively low (*ca.* 30). In the more SiO_2-undersaturated LAMP varieties the leucite molecule appears in the norm. Mg# varies between 57 and 71 and the highest values (*ca.* 80) correspond to the picritic lamprophyres. The alnöite presents larnite in the norm (*Cs*), which is one characteristic of such SiO_2-deficient, Ca-rich igneous rock. Calcite and magnesite molecules reflect the high CO_2 content of some LAMP.

The triangular plot MgO-Al_2O_3-FeO* (Fig. 2) well discriminates BAS from LAMP and the several LAMP varieties. BAS present the lowest MgO contents and contrast with the high MgO contents of the picritic lamprophyres. Among LAMP, monchiquites are chemically indistinguishable from camptonites (*cf.* Rock, 1979), but the biotite lamprophyres (including the alnöite) and the picritic lamprophyres define distinct fields.

Similar differences are seen in major oxides *vs.* Mg# diagrams (Fig. 3). SiO_2, Al_2O_3, Na_2O and K_2O contents are higher and FeO_t, MgO and CaO are lower for BAS when compared to LAMP. TiO_2, MnO and P_2O_5 differences between BAS and LAMP are not as clearly distinctive. Among LAMP these oxides are the least concentrated in the picritic varieties, along with Al_2O_3, FeO_t, Na_2O and K_2O.

TRACE ELEMENTS

Trace elements analyzed by ICP-MS (Australian National University) and NAA (Becquerel Laboratories, Australia) are listed in Table II. The plot Sm *vs.* (not normalized) La/Yb ratio (Fig. 4) shows a good discrimination for the different LAMP subgroups, especially the alnöite. BAS, on the other hand, plot in the fields for the monchiquites-camptonites.

In Figure 5, the normalized trace element variation diagrams for the different dike types were plotted using the primitive mantle values of Sun & McDonough (1989). P_2O_5 is used instead of P concentrations. BAS patterns (Fig. 5a) are charac-

TABLE I

Major elements by XRF and CIPW norms for BAS and LAMP (BLAMP = biotite lamprophyres; CAMP = camptonites; MONCH = monchiquites; CUM = picritic lamprophyres; ALNÖ = alnöite).

Sample (%)	B-3C BAS	B-3d(1) BAS	GPB-1-6 BAS	PS-1-1 BAS	B-2A BLAM	B-2C BLAM	C-1C BLAM	C-2B BLAM	C-2C BLAM	C-2D BLAM	PBF-1 BLAM
SiO_2	59.08	58.90	49.88	50.43	34.32	39.48	36.54	35.92	37.13	37.00	36.55
TiO_2	1.79	1.82	2.35	3.61	2.25	2.31	3.04	3.20	3.52	2.71	2.28
Al_2O_3	14.41	14.09	15.01	12.44	6.26	9.86	8.05	9.85	10.69	7.66	8.96
Fe_2O_3	8.15	8.30	11.61	15.74	13.79	12.51	14.14	13.65	13.74	13.29	12.24
MnO	0.13	0.14	0.20	0.20	0.20	0.18	0.19	0.20	0.17	0.19	0.16
MgO	1.80	1.91	2.86	3.35	17.37	12.03	14.39	12.03	10.31	15.33	14.99
CaO	3.78	4.27	6.10	7.08	10.83	12.41	13.47	13.69	13.37	13.60	12.09
Na_2O	3.79	3.52	4.01	3.11	0.58	2.14	0.62	1.77	2.38	0.49	0.80
K_2O	4.18	4.03	3.03	1.75	1.38	1.62	1.61	1.22	1.09	1.40	2.30
P_2O_5	0.70	0.73	1.06	0.64	0.47	0.55	0.38	0.58	0.60	0.36	0.46
Total	97.81	97.71	96.11	98.35	87.45	93.09	92.43	92.11	93.00	92.03	90.63
H_2O	0.53	1.14	2.11	0.56	11.47	5.61	4.84	5.82	5.77	5.75	5.92
CO_2	n.d.	n.d.	1.36	n.d	9.72	3.74	2.66	3.22	2.50	5.38	3.52
LOl	1.21	1.44	3.34	1.10	12.45	6.22	6.04	6.88	6.95	6.76	7.03
Mg#	30.43	31.31	32.79	29.65	71.38	65.57	66.84	63.58	59.78	59.55	70.81
S(ppm)	80	80	80	80	120	160	160	240	240	160	240
Cr(ppm)	4	1	1	14	1231	1376	1208	871	706	1218	1088
Q	9.74	10.86	0	4.15	0	0	0	0	0	0	0
C	0	0	0	0	4.41	0	0	0	0	0	0
Z	0.09	0.09	0.08	0.06	0.05	0.06	0.05	0.05	0.06	0.04	0.04
Or	25.48	24.6	18.86	10.7	9.48	10.43	0	4.74	7.03	9.13	7.92
Ab	33.02	30.7	35.67	27.12	5.69	9.56	0	0	1.21	4.56	0
An	10.32	11.13	14.77	15.29	0	13.62	15.83	16.88	16.66	16.03	16.67
Lc	0	0	0	0	0	0	8.21	2.52	0	0	5.7
Ne	0	0	0	0	0	5.48	3.12	8.92	11.22	0	4.08
Di	4.19	5.43	1.44	14.33	0	21.31	30.36	27.4	29.42	17.65	20.87
Wo	0	0	0	0	0	0	0	0	0	0	0
Hy	10.46	10.3	14.95	16.39	39.73	0	0	0	0	6.47	0
Ol	0	0	2.79	0	18.84	25.87	28.36	24.18	19.44	29.6	32.42
Cs	0	0	0	0	0	0	0.2	0	0	0	0
Mt	1.83	1.86	2.65	3.53	3.48	2.96	3.37	3.26	3.25	3.18	2.96
Cm	0	0	0	0	0.31	0.32	0.28	0.21	0.17	0.29	0.26
Il	3.5	3.56	4.69	7.07	4.95	4.77	6.33	6.68	7.28	5.66	4.82
Ap	1.74	1.81	2.67	1.57	1.3	1.42	0.99	1.52	1.56	0.94	1.22
Pr	0.02	0.02	0.02	0.02	0.03	0.03	0.03	0.05	0.05	0.03	0.05
Cc	0	0	3.12	0	21.43	8.56	6.07	7.36	5.73	12.28	8.04
Mag	0	0	0	0	0.67	0	0	0	0	0	0
Total	100.38	100.37	101.7	100.24	110.36	104.39	103.2	103.77	103.09	105.89	104.06

(to be continued)

TABLE I (Continuation)

Sample (%)	C-7A CAMP	C-7B1 CAMP	MV-2-B CAMP	PF-6B CAMP	GPG-1-5 MONCH	GPG-1-6A MONCH	GCB-9-2 CUM	GPA-8C2 CUM	GPA-8D CUM	A-01-A CAMP?	GPA-5 CAMP?	PCa-1 ALNÖ
SiO_2	40.44	41.36	40.64	38.36	38.09	40.62	44.31	34.47	37.97	40.41	36.80	34.38
TiO_2	2.46	2.64	3.14	2.62	2.25	2.37	1.21	0.84	1.01	1.39	1.98	1.93
Al_2O_3	10.76	11.26	12.00	10.18	8.54	10.38	8.52	5.01	7.61	9.71	11.84	9.92
Fe_2O_3	11.44	11.81	13.16	12.06	11.34	12.23	7.95	10.17	10.00	10.09	11.87	11.58
MnO	0.15	0.16	0.17	0.16	0.17	0.15	0.11	0.15	0.15	0.16	0.19	0.21
MgO	14.30	13.68	10.93	13.83	12.00	11.63	14.21	24.65	19.99	13.78	9.37	11.93
CaO	9.63	9.68	10.02	10.27	16.20	15.79	15.50	7.06	10.64	14.47	16.41	17.84
Na_2O	1.66	2.05	2.50	1.69	0.54	1.06	0.62	0.16	0.30	0.60	1.31	1.57
K_2O	1.77	1.75	1.56	1.68	0.88	0.93	0.90	0.25	0.70	1.13	1.53	0.94
P_2O_5	0.44	0.45	0.60	0.53	0.21	0.31	0.20	0.12	0.17	0.52	1.03	1.66
Total	93.05	94.84	94.72	91.38	90.22	95.47	93.53	82.88	88.54	92.26	92.33	91.96
H_2O	5.99	3.45	4.09	7.24	9.65	3.70	4.66	15.78	10.05	6.60	7.26	5.31
CO_2	5.24	2.72	2.22	6.20	5.66	2.00	2.70	8.58	5.62	5.00	6.34	1.90
LO_I	6.24	3.78	4.74	8.23	10.46	4.16	5.87	17.00	10.87	7.58	7.76	6.83
Mg#	71.23	69.64	62.19	69.43	67.70	65.32	77.97	82.76	79.83	73.01	60.99	67.11
S(ppm)	120	160	120	120	240	200	120	80	80	120	160	200
Cr(ppm)	713	665	379	599	580	386	1823	2568	1899	1002	280	404
Q	0	0	0	0	0	0	0	0	0	0	0	0
C	0.75	0	0	1.1	0	0	0	5.46	0	0	0	0
Z	0.04	0.05	0.06	0.05	0.03	0.03	0.03	0.02	0.02	0.04	0.06	0.07
Or	11.38	11.04	9.87	11.01	5.84	5.83	5.74	1.61	4.73	7.33	9.92	0
Ab	15.25	15.5	14.75	15.83	5.12	0.96	5.65	1.65	2.89	5.55	8.9	0
An	16.09	17.46	18.11	13.86	20.49	22.06	19.18	0	19.79	22.4	24.02	18.99
Lc	0	0	0	0	0	0	0	0	0	0	0	4.8
Ne	0	1.62	4.25	0	0	4.63	0	0	0	0	1.76	7.91
Di	0	11.17	14.12	0	26.12	37.38	36.09	0	2.99	16.93	14.86	18.09
Wo	0	0	0	0	0	0	0	0	0	0	0	0
Hy	17.19	0	0	14.83	11.25	0	13	53.52	29.86	18.36	0	0
Ol	23.87	30.7	25.35	25.81	15.93	18.33	12.04	22.33	27.45	16.52	23.06	26.81
Cs	0	0	0	0	0	0	0	0	0	0	0	10.26
Mt	2.7	2.74	3.06	2.9	2.76	2.82	1.86	2.7	2.48	2.4	2.83	2.77
Cm	0.17	0.15	0.09	0.14	0.14	0.09	0.42	0.67	0.47	0.24	0.07	0.1
Il	5.07	5.34	6.37	5.51	4.79	4.77	2.48	1.95	2.19	2.89	4.12	4.03
Ap	1.14	1.14	1.53	1.4	0.56	0.78	0.51	0.35	0.46	1.35	2.66	4.35
Pr	0.02	0.03	0.02	0.02	0.05	0.04	0.02	0.02	0.02	0.02	0.03	0.04
Cc	11.98	6.22	5.09	14.18	12.89	4.56	6.15	15.1	12.8	11.4	14.48	4.35
Mag	0	0	0	0	0	0	0	3.75	0	0	0	0
Total	105.67	103.17	102.67	106.64	105.97	102.26	103.17	109.32	106.16	105.43	106.78	102.56

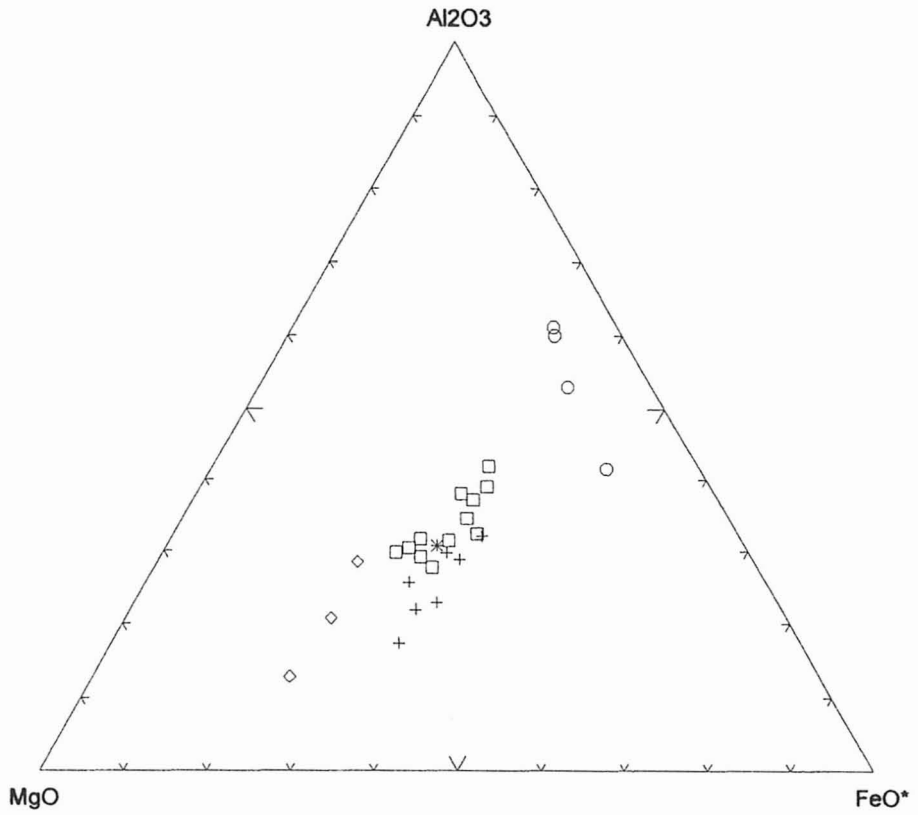

Fig. 2 — MgO-Al_2O_3-FeO* plot for the samples listed in Table I. ○ = basaltic dikes; ❑ = camptonites and monchiquites; + = biotite lamprophyres; ◊ = picritic lamprophyres; * = alnöite.

terized by average normalized La/Yb ratios [$(La/Yb)_N$] of *ca.* 16. Negative anomalies are found for Nb, Ta (high field strength elements) and Sr. Not all BAS samples present negative anomalies for P_2O_5.

Alnöite PCa-1 is compared to Rock's (1991) average values for this type of rock [$(La/Yb)_N$ = 42; Fig. 5b]. Two other LAMP samples (A-01-A e GPA-5) present a similar pattern, where Ba, Th, U, Nb, and Ta and in particular LREE (La, Ce, Pr, Nd) and Pb, Sr, P_2O_5 and Sm are present in higher concentrations as compared to BAS and other LAMP. These samples also show negative anomalies in Rb, K and Ti and intermediate HREE concentrations between BAS and other LAMP varieties. The other biotite lamprophyres (Fig. 5c) show $(La/Yb)_N$ = 31 and negative Rb, Th, U and K and positive Pb anomalies. As opposed to the alnöite pattern, other LAMP varieties show no Ti anomalies. The trace element patterns of the biotite lamprophyre group overlaps that of the monchiquite-camptonite group (Fig. 5d), but show lower $(La/Yb)_N$ (≅ 19).

Samples GPG-1-5 and GPG-1-6A (Fig. 5d) are intermediate between the monchiquite-camptonite and picritic lamprophyre patterns, notably in the P_2O_5 negative anomaly.

The picritic lamprophyre patterns (Fig. 5e) have the lowest $(La/Yb)_N$ (≅ 10) of all dikes and are also characterized by the lowest abundances in the incompatible elements Rb, Ba and Th.

RADIOGENIC ISOTOPES

Table III presents K-Ar data compiled from the literature and recalculated according to the recommendations in Steiger & Jaeger (1977). The numbers are not conclusive concerning the age of the dike manifestations. For example, Ponta do Surutuva data correspond to samples collected from

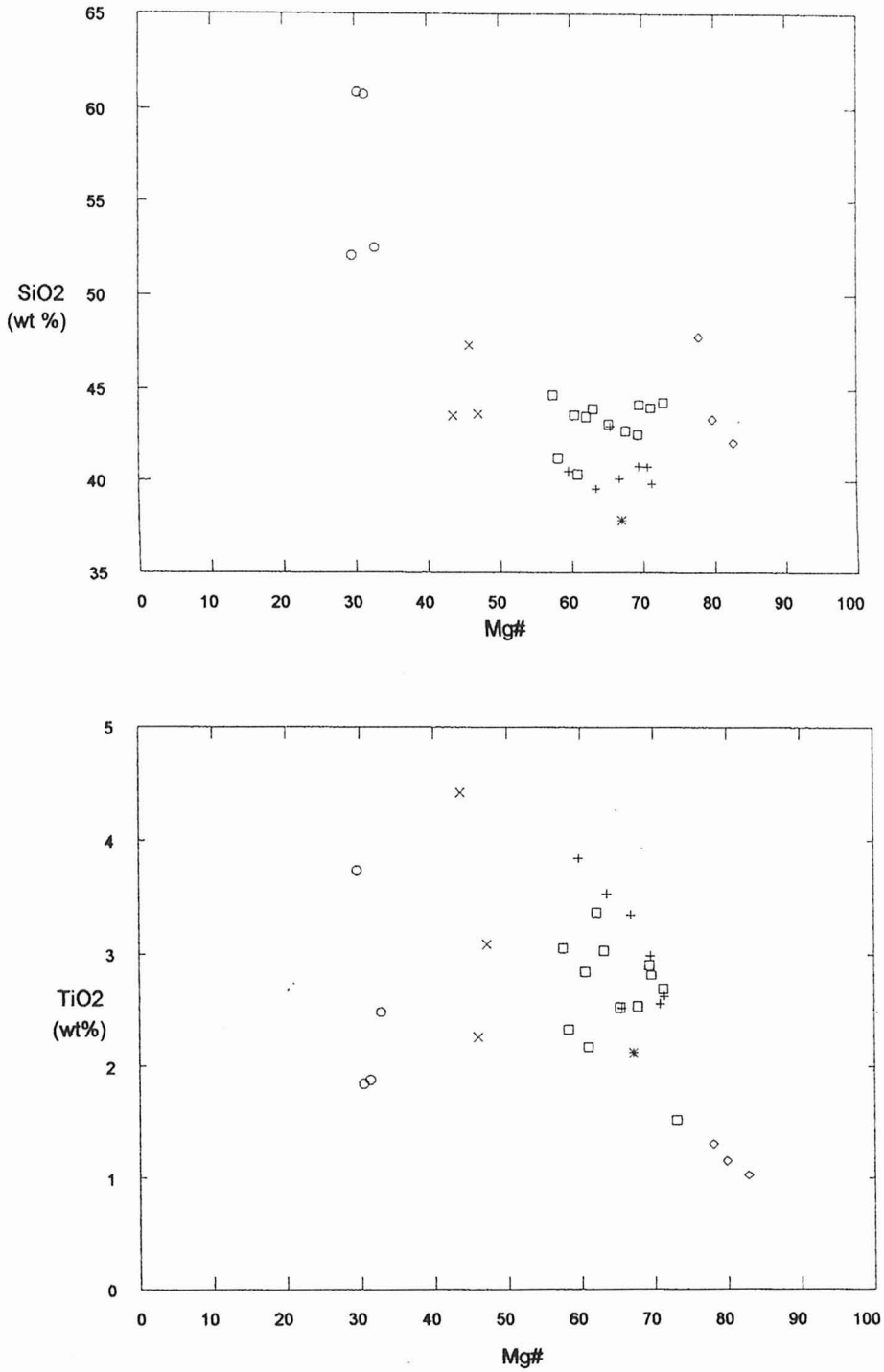

Fig. 3a — Major oxides *vs.* Mg# (= MgO/(MgO + 0.85 FeO* + Fe_2O_3) plot for the samples listed in Table I. See Fig. 2 for description of symbols.

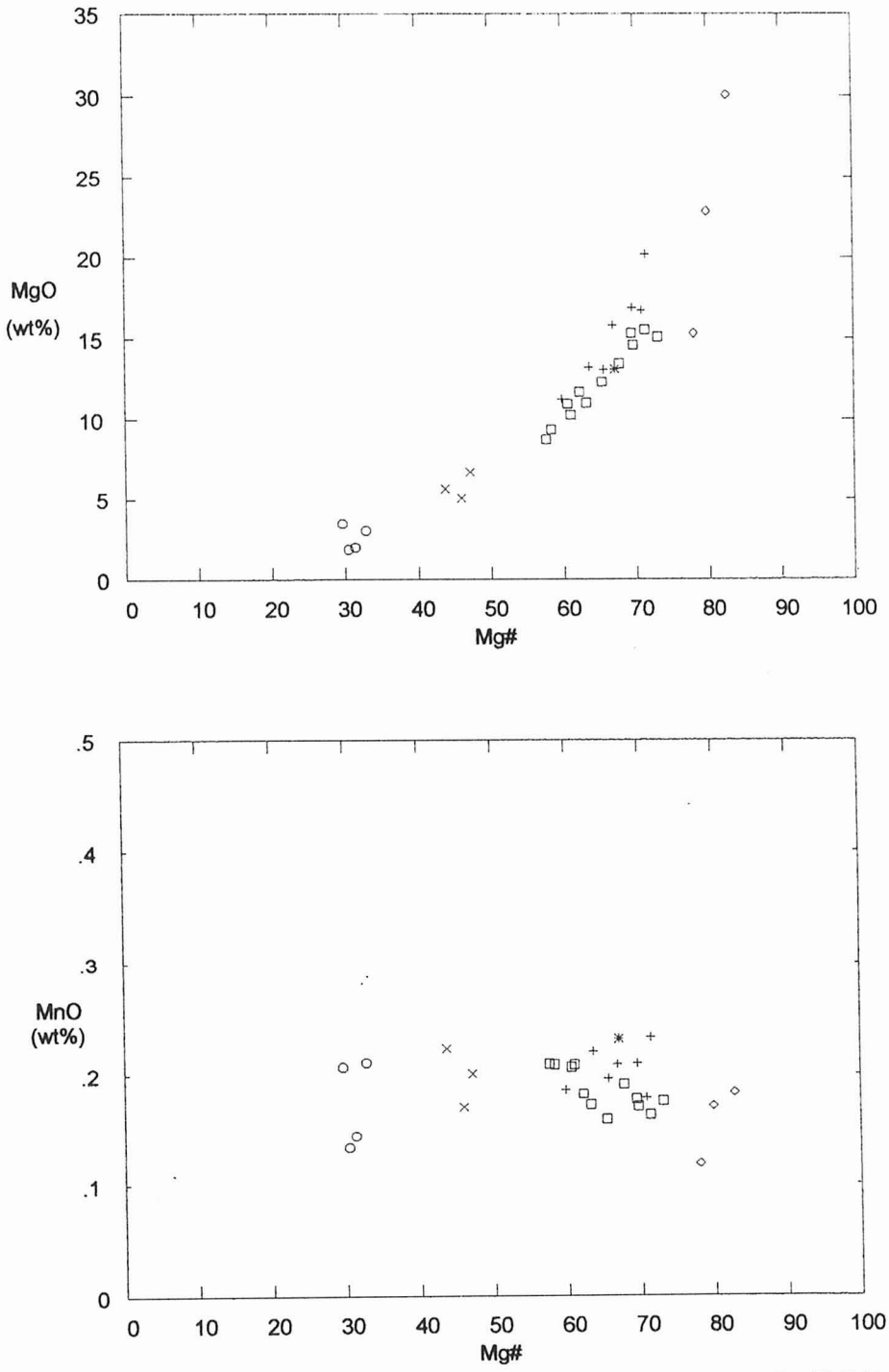

Fig. 3b — Major oxides *vs.* Mg# (= MgO/(MgO + 0.85 FeO* + Fe_2O_3) plot for the samples listed in Table I. See Fig. 2 for description of symbols.

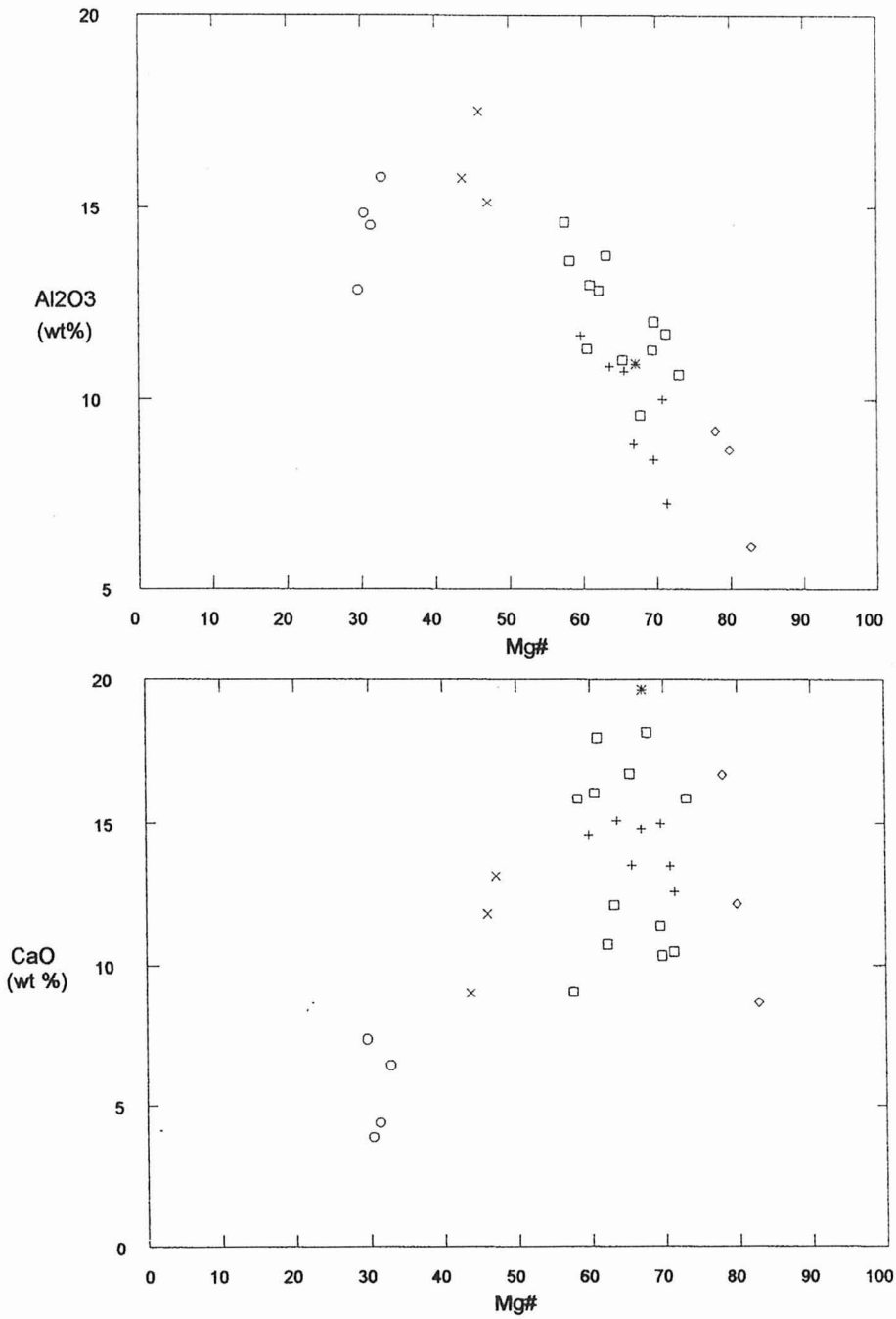

Fig. 3c — Major oxides *vs.* Mg# (= MgO/(MgO + 0.85 FeO* + Fe_2O_3) plot for the samples listed in Table I. See Fig. 2 for description of symbols.

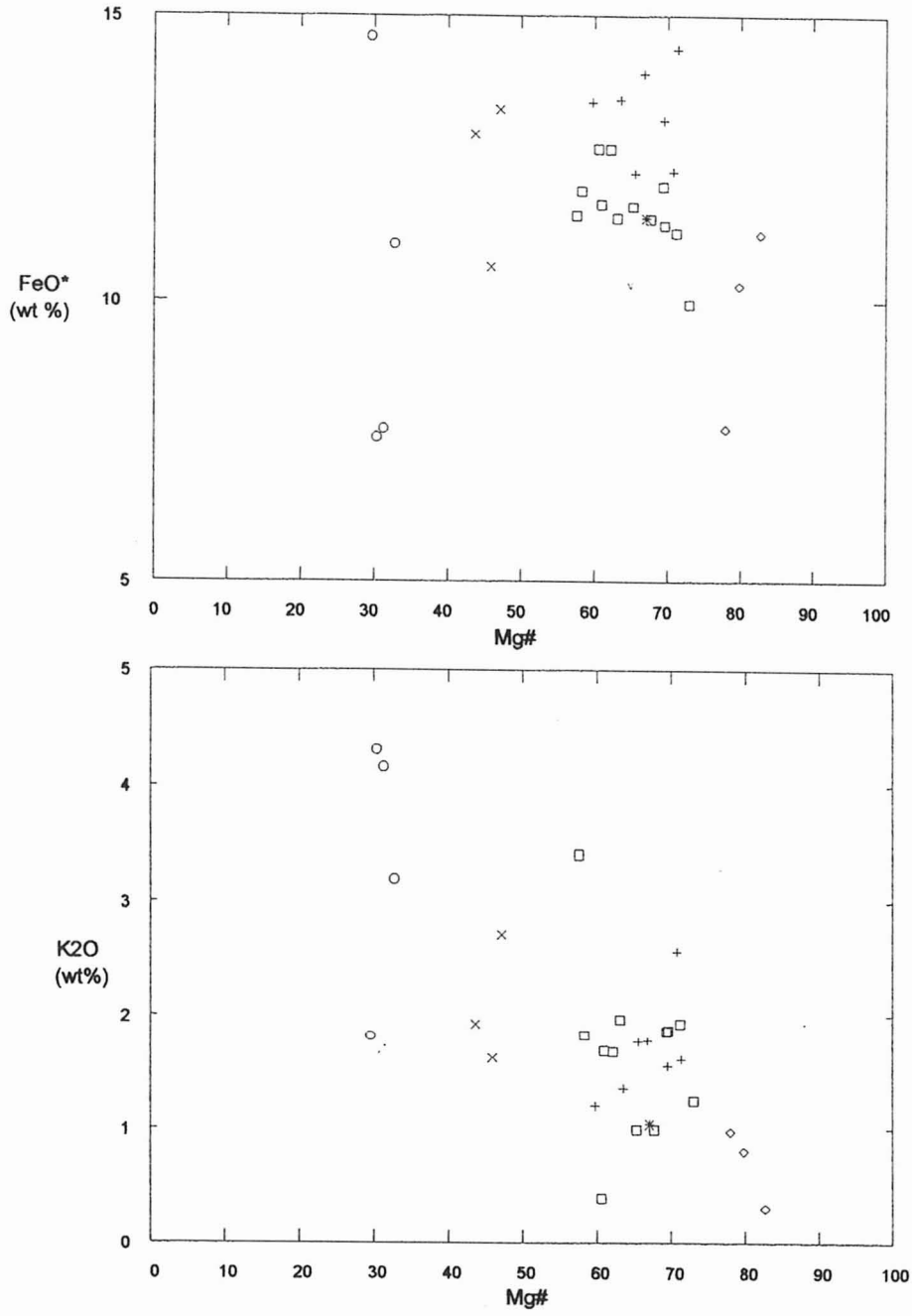

Fig. 3d — Major oxides *vs.* Mg# (= MgO/(MgO + 0.85 FeO* + Fe_2O_3) plot for the samples listed in Table I. See Fig. 2 for description of symbols.

he borders to the core of one dike, and fall in the broad 128-144 Ma interval. The Toninhas dike hows a scatter from 133 Ma to 148 Ma. However, he K-Ar data points to a 130 Ma age for BAS, vhich is the average age of the Paraná Basin ba-alts (*cf.* 125 Ma age for porphyry diorite and diorite samples that may have come from the Natividade da Serra-Caraguatatuba region).

Table IV presents $^{87}Sr/^{86}Sr$ and calculated $^{87}Rb/^{86}Sr$ from Rb and Sr concentrations. The Sr isotopes were measured by thermal ionization mass spectrometry at the Department of Terrestrial

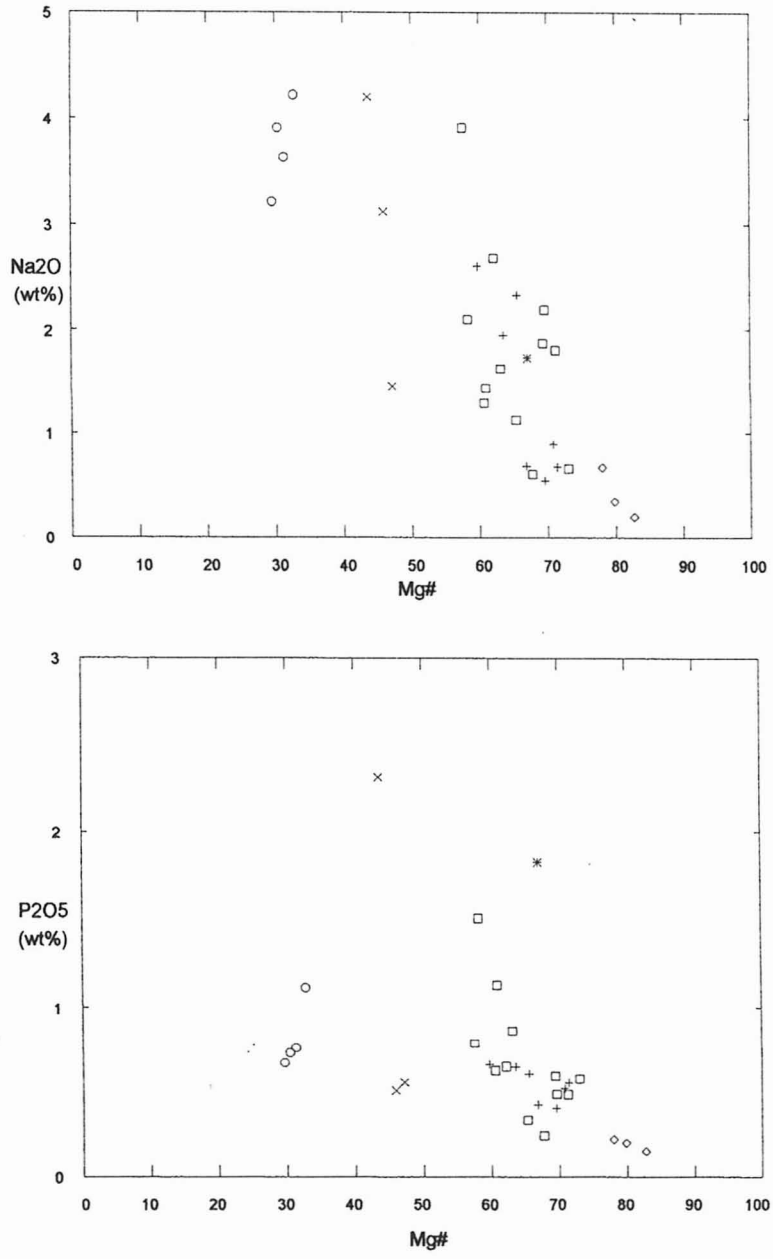

Fig.. 3e — Major oxides *vs.* Mg# (= MgO/(MgO + 0.85 FeO* + Fe_2O_3) plot for the samples listed in Table I. See Fig. 2 for description of symbols.

Magnetism of the Carnegie Institution of Washington (DTM-CIW, U.S.A.) and at the Centre for Isotope Studies (CSIRO, Sydney, Australia). When Rb-Sr data are plotted in the $^{87}Sr/^{86}Sr$ *vs.* $^{87}Rb/^{86}Sr$ diagram (Fig. 6), BAS data cluster around a 130 Ma isochron (initial $^{87}Sr/^{86}Sr$ ratio = 0.7066). Two samples from São Sebastião Island plot on a 80 Ma isochron (initial $^{87}Sr/^{86}Sr$ ratio = 0.7042), which is the age of the alkaline intrusions in the island (see Ulbrich & Gomes, 1981). For LAMP, the best fit is 116 Ma (initial $^{87}Sr/^{86}Sr$ ratio = 0.7055) and the isochron is defined by the samples PCa-1, A-01-A and GPA-5 and the biotite lamprophyres. The 116 Ma age suggests that LAMP is

TABLE II

BAS and LAMP trace element data analysed by ICP-MS and NAA.
See Table I for abbreviations (n.d. = elements not analysed by NAA).

Sample (ppm)	B-3C BAS	B-3d(1) BAS	GPB-1-6 BAS	PS-1-1 BAS	B-2A BLAM	B-2C BLAM	C-1C BLAM	C-2B BLAM	C-2C BLAM	C-2D BLAM	PBF-1 BLAM
Cs	2.39	2.46	0.88	2.18	1.50	9.03	1.42	3.12	2.03	0.49	1.97
Rb	112	112	71	108	57	62	78	56	45	75	110
Ba	1270	1186	932	654	1001	1170	857	1094	1710	849	801
Th	12.60	12.79	7.54	5.88	4.65	7.77	5.77	8.82	8.42	5.56	5.73
U	n.d.	2.98	n.d.	1.39	n.d.	n.d.	n.d.	n.d.	n.d.	n.d.	n.d.
Nb	40.0	63.2	57.0	34.5	73.0	71.0	57.0	66.0	66.0	51.0	59.0
Ta	3.94	3.65	3.86	2.04	3.47	4.65	4.33	5.24	4.80	3.05	3.61
La	82.2	86.9	60.0	48.0	60.5	72.0	49.5	64.8	66.7	43.1	44.1
Ce	179	173	131	106	120	148	98	132	135	89	91
Pb	16	15	12	9	3	12	8	13	7	11	9
Pr	n.d.	22.1	n.d.	13.5	n.d.	n.d.	n.d.	n.d.	n.d.	n.d.	n.d.
Sr	928	777	854	464	734	1031	744	1062	1070	528	737
Nd	80.1	84.5	66.8	55.6	53.9	59.2	50.2	58.1	61.4	44.9	45.5
Sm	16.0	15.5	13.5	11.8	9.9	10.1	9.4	10.7	11.2	8.0	8.5
Zr	444	523	366	346	229	261	217	237	254	190	183
Hf	12.0	12.2	8.3	8.4	5.3	5.6	5.3	4.8	5.2	4.9	4.0
Eu	5.00	4.25	4.13	3.31	2.69	2.78	2.80	3.17	3.30	2.37	2.52
Gd	n.d.	12.2	n.d.	10.8	n.d.	n.d.	n.d.	n.d.	n.d.	n.d.	n.d.
Tb	1.91	1.82	1.65	1.69	1.07	1.02	1.02	1.07	1.30	0.70	1.02
Dy	9.10	8.77	8.60	8.80	5.40	5.30	5.00	5.10	6.50	3.20	5.10
Li	n.d.	16.7	n.d.	12.0	n.d.	n.d.	n.d.	n.d.	n.d.	n.d.	n.d.
Y	32.0	44.4	33.0	44.1	52.0	42.0	45.0	37.0	38.0	43.0	53.0
Ho	1.61	1.60	1.62	1.71	1.01	0.91	0.79	0.96	1.05	0.59	0.87
Er	n.d.	4.09	n.d.	4.47	n.d.	n.d.	n.d.	n.d.	n.d.	n.d.	n.d.
Yb	3.08	3.24	2.86	3.64	1.38	1.63	1.17	1.31	1.54	0.98	1.12
Lu	0.47	0.46	0.39	0.52	0.16	0.18	0.15	0.15	0.18	0.12	0.15
Ga	n.d.	25	n.d.	22	n.d.	n.d.	n.d.	n.d.	n.d.	n.d.	n.d.
(La/Yb)N	19.2	19.2	15.1	9.5	31.5	31.7	30.4	35.5	31.1	31.6	28.3

(to be continued)

an intermediate event between BAS and the São Sebastião Island alkaline magmatism. The LAMP samples that do not fall on the 116 Ma isochron might define lines of mixture or derivation.

Distinct mantle sources for BAS and LAMP are indicated by preliminary Sr, Nd and Pb isotopic data (not age-corrected) by thermal ionization mass spectrometry (DTM-CIW, U.S.A.). BAS have $\varepsilon_{Nd}(i)$ of –5 and initial $^{87}Sr/^{86}Sr$ of 0.706 to 0.707, falling between values for the low- and high-Ti Paraná Basalt suite (Fig. 7). In contrast, samples from LAMP show $\varepsilon_{Nd}(i)$ between +1 and +2 and $^{87}Sr/^{86}Sr$ of around 0.705, close to Tristan-Walvis Ridge/Group I kimberlite fields.

Except for the alnöite PCa-1, the measured $^{206}Pb/^{204}Pb$ ratios for BAS and LAMP scatter in the 18.21-18.71 interval. However, age-corrected values for this same sample (assuming 116 Ma) brings it down to the cluster of LAMP samples. All samples lie above Hart's (1984) North Hemisphere

TABLE II (Continuation)

Sample (ppm)	C-7A CAMP	C-7B1 CAMP	MV-2-B CAMP	PF-6B CAMP	GPG-1-5 MONCH	GPG-1-6A MONCH	GCB-9-2 CUM	GPA-8C2 CUM	GPA-8D CUM	A-01-A CAM?	GPA-5 CAMP?	PCA-1 ALNÖ
Cs	0.97	0.49	2.16	0.49	1.00	1.94	1.26	1.05	1.12	3.14	3.97	1.98
Rb	37	46	51	38	22	24	29	11	25	46	58	29
Ba	765	853	925	741	254	410	256	176	225	387	795	1223
Th	4.45	4.17	4.24	5.13	1.98	2.80	1.57	1.06	1.48	2.71	3.86	19.07
U	n.d.	n.d.	1.01	n.d.	0.59	0.80	n.d.	n.d.	n.d.	0.99	1.27	7.12
Nb	57.0	56.0	52.0	61.0	30.7	43.5	21.0	34.0	28.0	25.3	48.4	92.2
Ta	2.91	3.55	2.94	2.87	1.88	2.50	0.86	0.93	2.00	1.56	2.93	5.54
La	32.6	35.4	43.4	43.1	21.0	28.3	15.8	9.9	12.4	32.8	56.6	152.6
Ce	67	72	91	86	48	63	34	21	28	71	120	275
Pb	13	6	3	7	3	3	7	3	16	3	4	9
Pr	n.d.	n.d.	11.5	n.d.	6.5	8.1	n.d.	n.d.	n.d.	8.9	14.9	30.0
Sr	725	872	1159	871	428	430	322	226	244	624	1164	1715
Nd	37.7	36.5	46.7	42.9	27.6	33.5	19.5	11.9	14.7	36.0	58.5	108.2
Sm	7.1	7.6	9.6	8.8	6.1	7.0	4.7	2.7	3.6	7.3	10.8	17.7
Zr	198	211	278	229	154	168	117	86	105	159	270	331
Hf	4.2	4.6	5.8	5.3	4.7	4.7	2.9	1.8	2.3	3.6	5.2	6.0
Eu	2.10	2.37	2.99	2.81	1.83	2.14	1.49	0.81	1.06	2.22	3.25	4.99
Gd	n.d.	n.d.	8.0	n.d.	5.3	6.0	n.d.	n.d.	n.d.	6.3	8.9	13.0
Tb	0.73	0.80	1.18	1.18	0.77	0.88	0.65	0.35	0.43	0.96	1.31	1.86
Dy	3.90	4.29	5.50	6.20	3.75	4.28	3.40	1.93	2.34	4.74	6.25	8.21
Li	n.d.	n.d.	11.4	n.d.	82.7	37.5	n.d.	n.d.	n.d.	28.8	47.9	52.5
Y	30.0	32.0	26.2	35.0	17.5	20.0	35.0	19.0	27.0	23.5	29.9	38.6
Ho	0.68	0.72	0.96	1.24	0.66	0.76	0.63	0.34	0.44	0.88	1.14	1.45
Er	n.d.	n.d.	2.23	n.d.	1.60	1.86	n.d.	n.d.	n.d.	2.25	2.90	3.51
Yb	1.12	1.18	1.56	1.41	1.17	1.37	1.12	0.67	1.10	1.75	2.24	2.58
Lu	0.11	0.16	0.21	0.18	0.17	0.19	0.14	0.08	0.15	0.25	0.32	0.36
Ga	n.d.	n.d.	26	n.d.	32	33	n.d.	n.d.	n.d.	28	25	30
(La/Yb)N	20.9	21.5	20.0	21.9	12.9	14.9	10.1	10.6	8.1	13.4	18.1	42.4

Reference Line (NHRL) on plots of $^{208}Pb/^{204}Pb$ *vs.* $^{206}Pb/^{204}Pb$ (graph not presented), but only BAS are distinctly above the NHRL in $^{207}Pb/^{204}Pb$ *vs.* $^{206}Pb/^{204}Pb$, falling close to the Low-Ti Paraná basalt suite (Fig. 8). In general, LAMP Pb isotopic data are closer to the Tristan-Walvis Ridge/Group I kimberlite fields.

Isotopic compositions of LAMP indicate a deeper mantle source with greater proportions of asthenospheric-derived melts than, for example, the alkaline suite of the margins of the São Francisco Craton (Carlson *et al.*, 1993), which presents Enriched Mantle I (EM-I) isotopic characteristics ($-8 < \varepsilon_{Nd}(0) < -3.3$, $^{87}Sr/^{86}Sr = 0.7050\text{-}0.7066$, $17.40 < ^{206}Pb/^{204}Pb < 19.98$, $^{207}Pb/^{204}Pb$ falling on NHRL but $^{208}Pb/^{204}Pb$ well above the NHRL).

DISCUSSION

Piccirillo *et al.* (1988b) summarized the principal aspects of the Paraná Basin basalts (Serra Geral Formation) as follows. The low-Ti basalts of the Southern portion of the Paraná Basin (SPB) are characterized by 65% in volume of tholeiitic basalts, 22% of tholeiitic andesites or intermediate

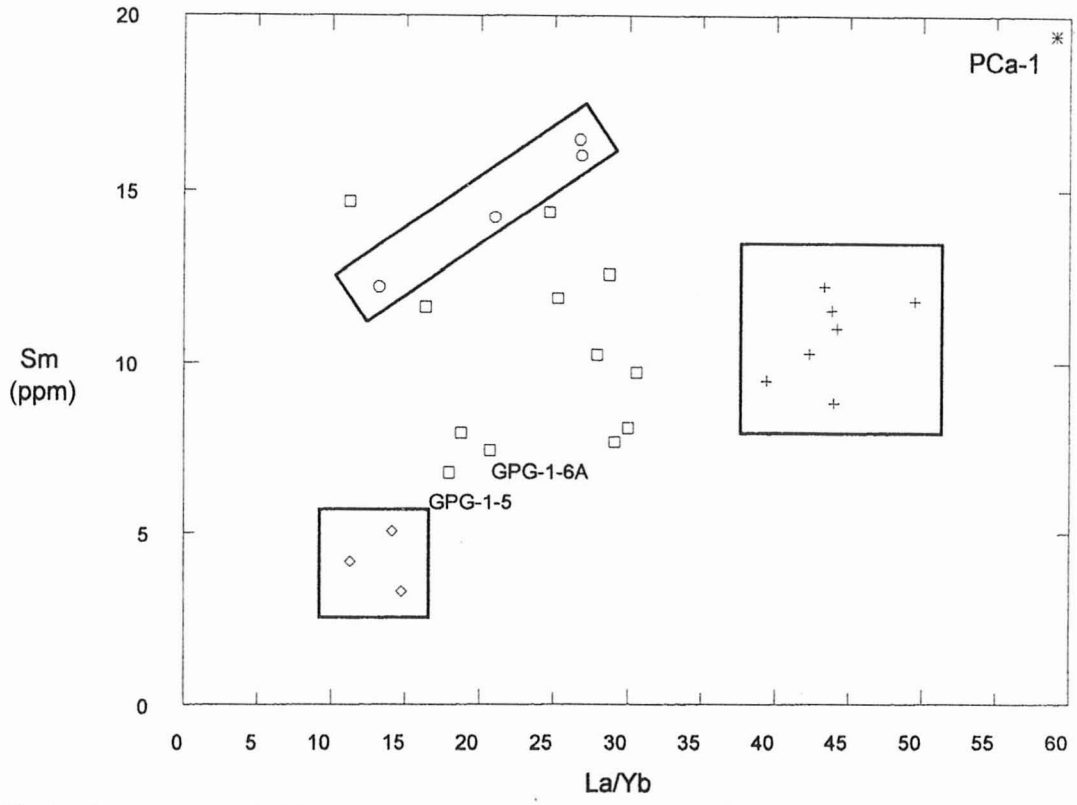

Fig. 4 — Sm *vs.* (not normalized) La/Yb ratios for BAS and LAMP. Two monchiquites are indicated for reference.

volcanics and 13% of Palmas-type porphyritic acid volcanics. The high-Ti basalts of the Northern portion of the Paraná Basin (NPB) are predominantly tholeiitic basalts. Acid porphyritic lavas are rare (Chapecó-type). No intermediate volcanics were found in NPB. The Ti-intermediate basalts of the central portion of the Paraná Basin (CPB), located between the Uruguay and Piquiri River Lineaments, are considered by Bellieni *et al.* (1986) as a transitional zone between the other two.

The Paraná Basin basalts are evolved rocks (Mg# < 56%; Piccirillo *et al.*, 1988b). Crystal fractionation alone would not be enough to explain the generation of high-Ti basalts from low-Ti basalts. Partial melting (higher for the low-Ti and lower for the high-Ti basalts), or mantle heterogeneities, could have generated each group and crustal contamination could explain the absence of rocks of intermediate compositions in CPB and NPB. The generation of more acid melts would require higher temperatures, next or in the base of the crust during the general process of crustal thinning and close to the plate generation zone.

Comin-Chiaramonti *et al.* (1983) suggested that the higher contents of TiO_2, P, Zr, Ba, Sr and Rb of the dikes from Peruíbe-Rio de Janeiro were formed in a peripheral zone (east portion of the Paraná Basin), where the degree of melting would be lower in relation to the areas of higher thermal anomalies.

The mafic dikes of the Ponta Grossa Arch also present similarities with the basaltic floods of CPB and NPB (Piccirillo *et al.*, 1988b) and correlate with similar occurrences related to the Etendeka (SW Africa) and Lebombo (SE Africa) basins. Montes-Lauar *et al.* (1990) showed that some of the São Sebastião Island dikes also present affinities with the high-Ti Paraná basalts.

Regarding the dikes of this study, BAS seem to have some of the petrological and geochemical characteristics as the high-Ti basalts of the Paraná Basin and the mafic dikes of the Ponta Grossa

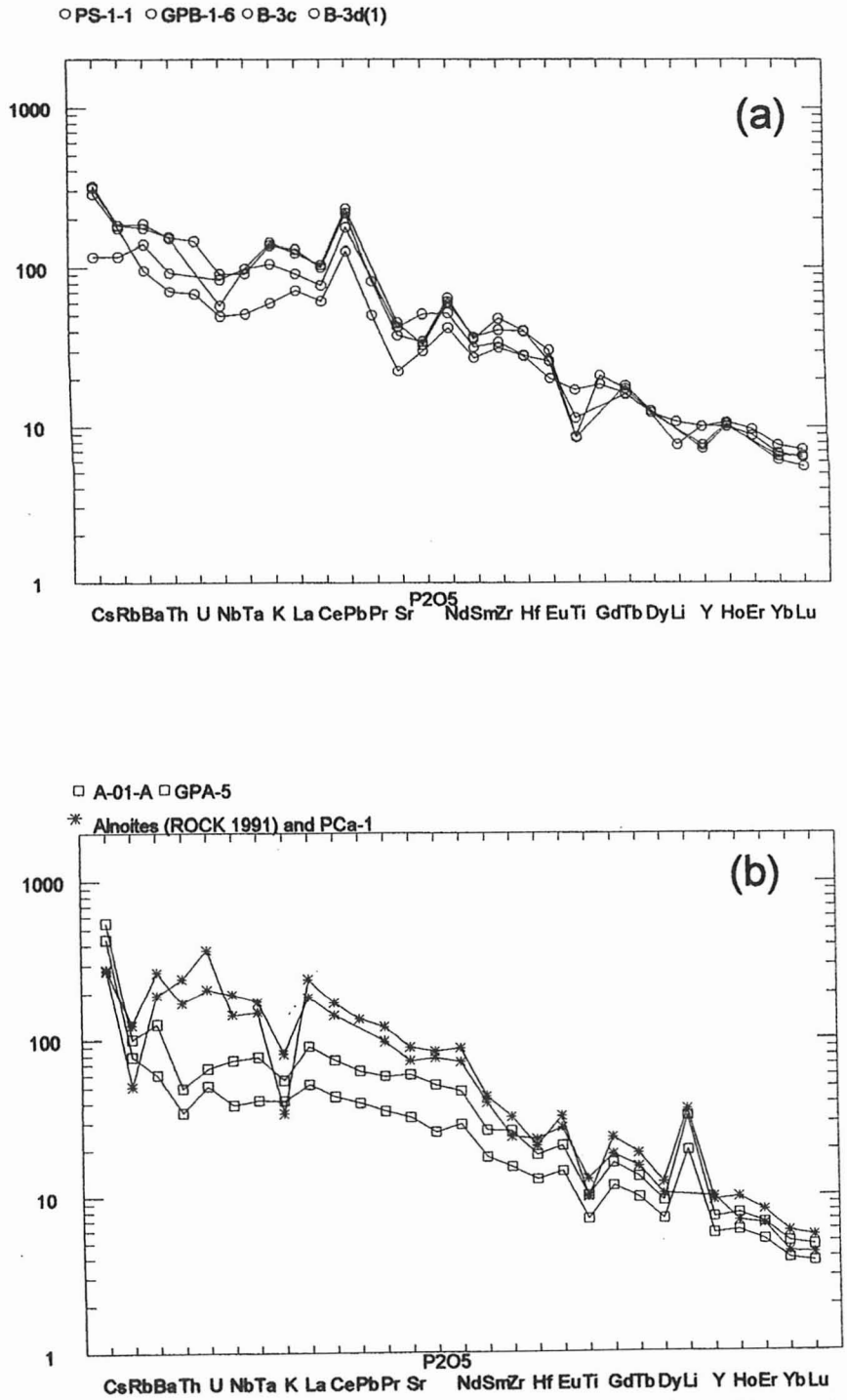

Fig. 5 — Multielement diagrams, using Sun & McDonough's (1989) primitive mantle normalization values (P substituted for P_2O_5). (a) BAS; (b) Rock's (1991) alnöite, PCa-1, A-01-A and GPA-5.

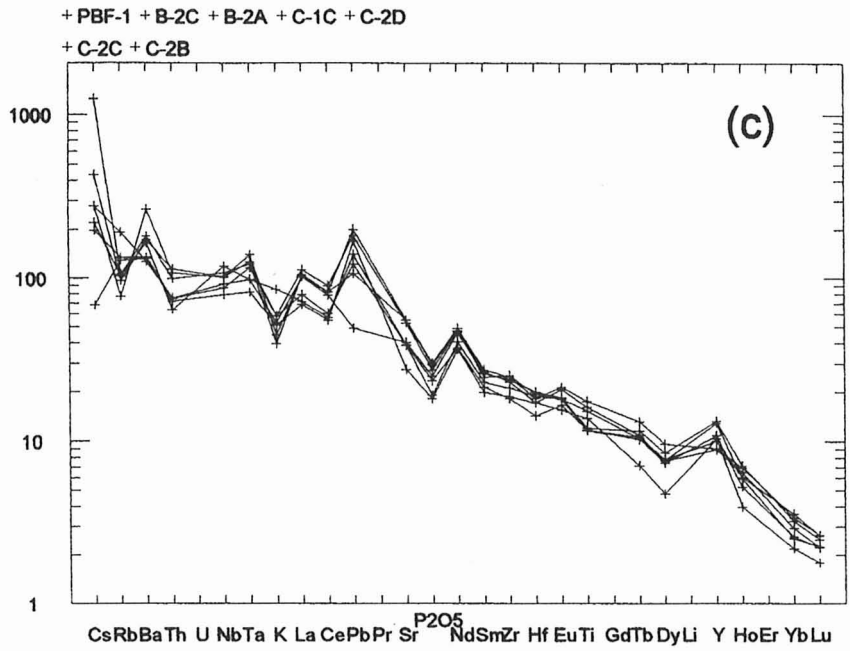

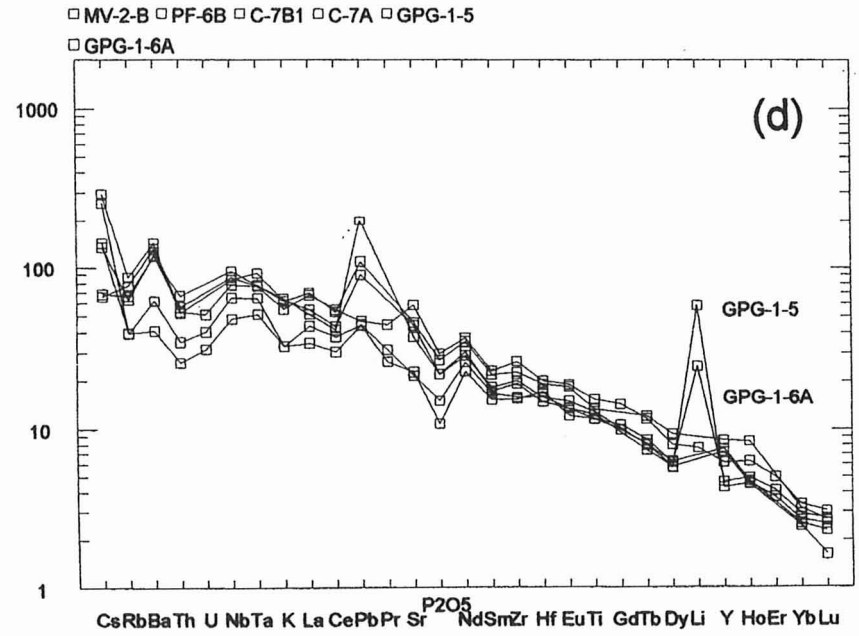

Fig. 5 — Multielement diagrams, using Sun & McDonough's (1989) primitive mantle normalization values (P substituted for P_2O_5). (c) biotite lamprophyres; (d) monchiquites-camptonites.

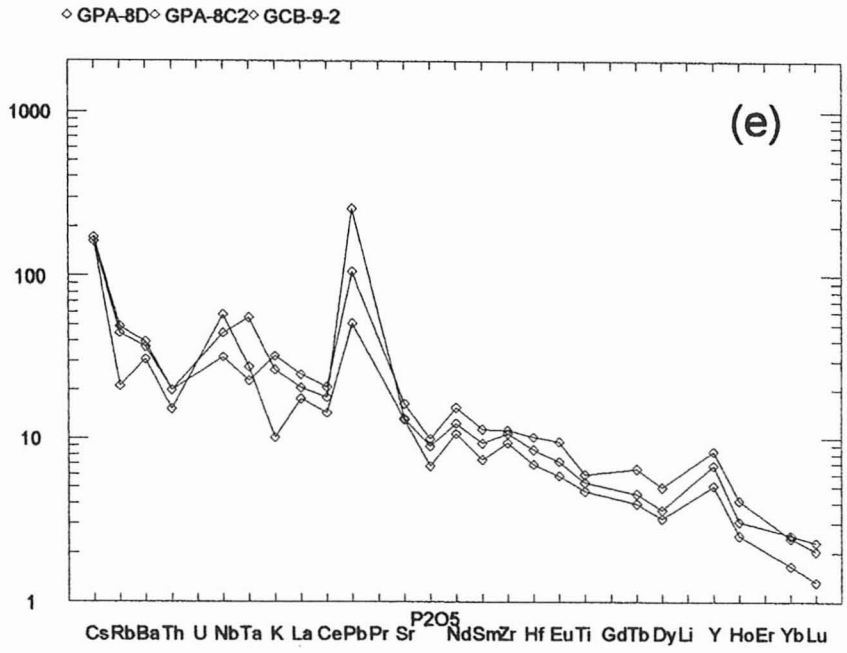

Fig. 5 — Multielement diagrams, using Sun & McDonough's (1989) primitive mantle normalization values (P substituted for P_2O_5). (e) picritic lamprophyres.

Arch. However, the magmatic event that resulted in the formation of the variety of LAMP dikes (picritic, biotite and camptonite-monchiquite lamprophyres) surely represents a transition towards magmas of alkaline and possibly carbonatitic affinity, as shown by mineral analyses, major, trace element and isotopic data.

If further studies confirm the suggested 116 Ma age for LAMP magmatism, then at least two major alkaline events took place in the São Sebastião-Ubatuba region: a dike suite of mafic-ultramafic lamprophyres genetically related to carbonatitic manifestations which evolved from picritic to monchiquitic-camptonitic types that is followed (at about 80 Ma) by the intrusive alkaline magmatism in the São Sebastião, Búzios and Vitória islands, represented by major nordmarkites and pulaskites and minor alkaline gabbro and pyroxenite cumulates.

Ulbrich *et al.* (1991), discussing K-Ar data for alkaline rocks from Southern Brazil and Eastern Paraguay, separated four chronogroups (133, 108, 84 and 70-62 Ma). At the Ponta Grossa Arch 133, 108 and 84 Ma old alkaline rocks occur. In the Rio de Janeiro-São Paulo coastal belt, magmatic pulses took place at 133 and 84 Ma. Jacupiranga (130 Ma) and Juquiá (127 Ma) carbonatite complexes belong to the oldest chronogroup. If a distinct 116 Ma lamprophyre activity took place, a much more complex tectonomagmatic situation arises where distinct basaltic and alkaline magmatic pulses operated at distinctive time events, pointing, in addition, to distinct mantle sources for the magma generation of each event.

ACKNOWLEDGEMENTS

Gianna Garda wishes to thank Prof. D. I. Groves and Dr. B. J. Griffin for SEM facilities at the University of Western Australia, Dr. N. Pearson for electron microprobe facilities at Macquarie University, Drs. I. Campbell and S. Eggins for ICP-MS trace-element analyses (Australian National University), Dr. H. Cauldron for NAA rare-element analyses (Becquerel Laboratories) Prof. S. Y. O'Reilly and Geoff Denton for Sr isotope analyses at the CSIRO (Sydney, Australia) and CAPES (Proc. 1798/93) for financial support during her stay in Australia.

TABLE III

K-Ar data compiled from the literature and recalculated according to the recommendations in Steiger & Jaeger (1977).

Locality	Sample			%K	Ar_{40} rad	Ar_{40} atm	Recalculated age (Ma)	Original age (Ma)	Error (*)	Reference
Ponto do Surutuva	SPK-0072	diabase (rim A)	WR	1.698	9.62		140.2	136.9	11.0	1
	SPK-0072R			1.701	9.8		142.4	139.4	11.2	1
	SPK-0060	diabase (5m from A)	WR	1.757	10		140.8	136.8	10.9	1
	SPK-0060R			1.775	9.9		138.1	135.4	10.8	1
	SPK-0062	diabase (10m from A)	WR	1.893	10.64		139.1	135.4	10.8	1
	SPK-0062R			1.907	10.74		139.4	136.6	10.9	1
	SPK-0150	diabase (10m from A)	feldspar	2.65	13.97		130.8	127.2	10.2	1
	SPK-0150R			2.661	14.59		135.8	132.6	10.6	1
	SPK-0150R2			2.673	15.58		144.0	141.3	11.3	1
	SPK-0063	diabase (core)	WR	1.85	10.09		135.1	131.4	10.5	1
	SPK-0063R			1.855	9.67		129.4	126.3	10.1	1
	SPK-0063R2			1.859	9.49		126.8	123.9	9.9	1
	SPK-0063R3			1.863	9.5		126.6	124.1	9.9	1
	SPK-0193	diabase (core)	feldspar	2.646	13.9		130.3	126.7	10.1	1
	SPK-0193R			2.675	13.78		127.9	125.6	10.0	1
Toninhas	SPK-0179	diabase (rim A)	WR	1.453	8.71		148.0	144.6	11.6	1
	SPK-0028	diabase (5m from A)	WR	1.882	10.31		135.7	132.6	10.6	1
	SPK-0033	diabase (10m from A)	feldspar	3.565	19.41		134.9	131.8	10.5	1
Domingos Dias	SPK-0024	diabase (rim A)	WR	1.954	11.11		140.6	137.4	11.0	1
	SPK-0024R			1.943	11.1		141.3	137.3	11.0	1
	SPK-0023	diabase (20cm from A)	WR	2.319	14.08		149.8	146.3	11.7	1
	SPK-0023R			2.325	15.11		159.9	156.4	12.5	1
Praia de Santa Rita	SPK-0065	diabase (rim A)	WR	1.904	10.24		133.3	130.0	10.4	1
	SPK-0066	diabase (1m from A)	WR	1.925	10.08		129.9	126.9	10.2	1
Prainha		lamprophyre						132.4		4
Ponta do Bonete	SPK-0671	microporphyritic basalt	WR	2.06	11.1	7.5	133.5	130.9	5.1	2, 3
	SPK-0636	trachyandesite	WR	3.15	17.5	13.8	137.5	134.4	5.0	2, 3
	SPK-0678	trachyandesite	WR	3.15	17.5	14	137.5	134.7	5.0	2, 3
Praia Dura	SPK-0639	microporphyritic basalt	WR	2.37	12.8	5.2	133.8	131.0	5.0	2, 3
Toninhas?	SPK-0637	diabase	WR	1.85	9.9	10.5	132.7	131.0	5.0	2, 3
Praia Preta	SPK-0685	porphyry diorite	WR	2.94	14.3	13	121.0	118.0	4.7	2, 3
Km 129 da SP...	SPK-0583	porphyry diorite	WR	3.3	17.18	8.5	129.2	126.4	5.1	2, 3
Alto da Serra		diorite						124.5		4
Ilha de São Sebastião										
Costão do Encantado	SPK-0684	porphyry andesite	WR	3.61	18.2	16.8	125.2	122.6	5.0	2, 3
Água Branca	SPK-0683	microdiorite	WR	2.29	10.2	16.5	111.1	109.0	4.0	2, 3

References: 1. Amaral *et al.* (1966); 2. Minioli (1969); 3. Minioli *et al.* (1971); 4. Damasceno (1966); (*) Errors for reference (1) were calculated as 8% of original age (according to Amaral *et al.*, 1966).

TABLE IV

$^{87}Sr/^{86}Sr$ and $^{87}Rb/^{86}Sr$ data for BAS and LAMP. Samples analysed at CSIRO (Sydney, Australia), except those marked *, which were analysed at DTM-CIW (Washington, USA). See Table I for abbreviations (SSI = São Sebastião Island).

Sample	B-3C* BAS	B-3d(1) BAS	PS-1-1 BAS	PE-1B-2 BAS	PF-1B BAS	PPM-3* BAS	PPu-1 BAS	IB-10(e) SSI	IB-16-1 SSI
$^{87}Rb/^{86}Sr$	0.409	0.418	0.673	0.330	0.144	0.341	0.322	0.046	0.783
$^{87}Sr/^{86}Sr$	0.7078	0.7077	0.7078	0.7069	0.7065	0.7068	0.7071	0.7043	0.7056

Sample	B-2A BLAM	C-2D BLAMP	PBF-1* BLAMP	MV-2B CAMP	GPG-1-6A MONCH	GPA-8C2* CUM	A-01-A CAMP	GPA-5 CUM	PCa-1* ALNÖ
$^{87}Rb/^{86}Sr$	0.215	0.404	0.464	0.128	0.158	0.118	0.211	0.145	0.047
$^{87}Sr/^{86}Sr$	0.7059	0.7061	0.7059	0.7051	0.7052	0.7052	0.7058	0.7057	0.7056

TABLE V

Calculated $^{87}Sr/^{86}Sr(i)$ and $^{147}Sm/^{144}Nd$ and measured $^{143}Nd/^{144}Nd$, $^{207}Pb/^{204}Pb$ and $^{206}Pb/^{204}Pb$ ratios. Samples analysed at DTM-CIW (Washington, USA).

Sample		$^{87}Sr/^{86}Sr(i)$	$^{143}Nd/^{144}Nd(m)$	$^{147}Sm/^{144}Nd(c)$	$^{206}Pb/^{204}Pb(m)$	$^{207}Pb/^{204}Pb(m)$	$^{208}Pb/^{204}Pb(m)$
PPM-3	BAS	0.7062	0.5124	0.1265	18.30	15.57	38.50
B-3C	BAS	0.7070	0.5123	0.1202	n.d.	n.d.	n.d.
PF-6B	CAMP	n.d.	n.d.	n.d.	18.74	15.53	38.93
C-7A	BLAMP	0.7044	0.5126	0.1133	18.70	15.49	38.70
PBF-1	BLAMP	0.7052	0.5127	0.1079	18.21	15.52	38.57
PCa-1	ALNÖ	0.7055	0.5127	0.0976	19.94	15.64	39.68
PA-8C2	CUM	0.7050	0.5127	0.1263	18.71	15.59	38.08

REFERENCES

ALMEIDA, F. F. M., (1983), Relações tectônicas das rochas alcalinas mesozóicas da região meridional da Plataforma Sul-Americana. *Rev. Bras. Geoc.*, **13:** 139-158.

ALMEIDA, F. F. M.; HASUI, Y.; PONÇANO, W. L.; DANTAS, A. S. L.; CARNEIRO, C. R.; MELO, M. S. & BISTRICHI, C. A., (1981), *Mapa geológico do Estado de São Paulo, escala 1:500.000*. IPT-DMGA, VII, (Monografia 6).

AMARAL, G.; CORDANI, U. G.; KAWASHITA, K. & REYNOLDS, J. H., (1966), Potassium-argon dates of basaltic rocks from Southern Brazil. *Geochim. Cosmochim. Acta,* **30:** 159-189.

BELLIENI, G.; COMIN-CHIARAMONTI, P.; MARQUES, L. S.; MELFI, A. J.; NARDY, A. J. R.; PAPATRECHAS, C.; PICCIRILLO, E. M.; ROISENBERG, A. & STOLFA, D., (1986), Petrogenetic aspects of acid and basaltic lavas from the Paraná Plateau (Brazil): Geological, mineralogical and petrochemical relationships. *J. Petrol.*, **27:** 915-944.

BELLIENI, G.; MONTES-LAUAR, C. R.; DE MIN, A.; PICCIRILLO, E. M.; CAVAZZINI, G.; MELFI, A. J. & PACCA, I. G., (1990), Early and late cretaceous magmatism from São Sebastião Island (SE Brazil): geochemistry and petrology. *Geochim. Bras.*, **4:** 59-83.

CARLSON, R. W.; ESPERANÇA, S.; LAMBERT, D. D. & SVISERO, D. P., (1993), The EM-I component in the S. Atlantic: clues to its origin from isotopic and trace element data on Brazilian kimberlites. Trans. Amer. Geophys. Union (EOS), **74:** 633.

CHIEREGATI, L. A.; THEODOROVICZ, A. M. G.; THEODOROVICZ, A.; MENEZES, R. G.; CHIODI FILHO, C. & RAMALHO, R., (1982), *Projeto Folhas Natividade da Serra e Caraguatatuba*. SICCT-CPRM, vol. 1, 110p.

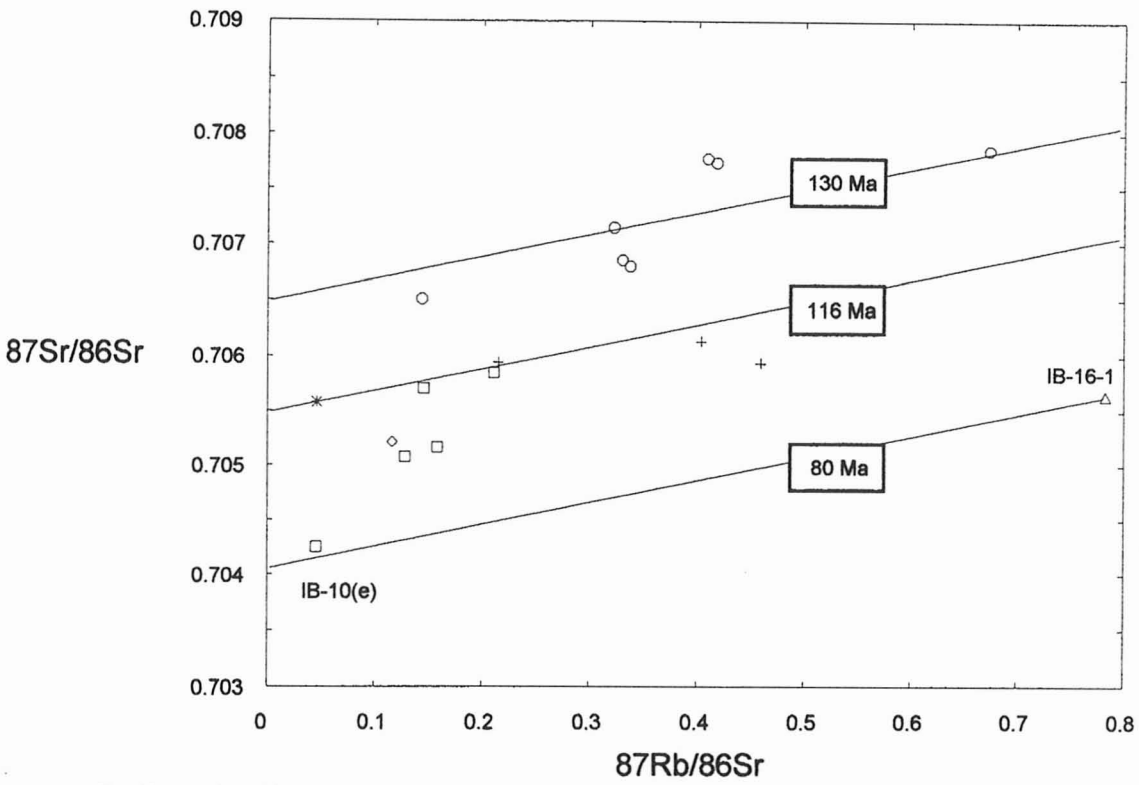

Fig. 6 — $^{87}Sr/^{86}Sr$ *vs.* $^{87}Rb/^{86}Sr$ diagram for the samples listed in Table IV. See Fig. 2 for description of symbols. A picrite [IB-10(e)] and a traquite [IB-16-1], as classified in the total alkalis *versus* silica diagram (e.g. Le Maitre 1989), are samples from São Sebastião Island.

CHIODI FILHO, C.; CHIEREGATI, L. A.; THEODOROVICZ, A. M. DE G.; THEODOROVICZ, A.; MENEZES, R. G. DE; RAMALHO, R. & BATOLLA JR., F., (1983), Geologia e recursos minerais das folhas Natividade da Serra e Caraguatatuba. *In*: Jornada Sobre a Carta Geológica do Estado de São Paulo em 1:50.000, 1. *Atas...* Pró-Minério/IPT, p. 8-26.

CLARKE, D., (1992), NEWPET: Shareware Program for geochemical data treatment.

COMIN-CHIARAMONTI, P.; GOMES, C. B.; PICCIRILLO, E. M. & RIVALENTI, G., (1983), High-TiO_2 basaltic dikes in the coastline of São Paulo and Rio de Janeiro States (Brazil). *N. Jahrb. Miner., Abbh.*, **146:** 133-150.

COUTINHO, J. M. V.; ENS, H. H.; RODRIGUES, E. P. & TASSINARI, C. C. G., (1991), Mafic dike swarms in the northern coast of São Paulo, Brazil (a preliminary report). *In*: International Symposium on Mafic Dikes, São Paulo, Brazil, 1991. *Extended Abstracts*: 111-115.

COUTINHO, J. M. V. & ENS, H. H., (1992), Diques lamprofíricos e diferenciados carbonatíticos da região de São Sebastião e Itanhaém – SP (resultados preliminares). *In*: Congresso Brasileiro de Geologia, 37, São Paulo, 1992. SBG-NSP, *Boletim de Resumos Expandidos*: 512-513.

DAMASCENO, E. C., (1966), Estudo preliminar dos diques de rochas básicas e ultrabásicas da região de Ubatuba, Estado de São Paulo. *An. Acad. bras. Ci.*, **38** (2): 293-304.

DAEE-UNESP, (1989), *Mapa geológico do Estado de São Paulo. Folha Santos, escala 1:250.000.*

DROOP, G. T. R., (1987), A general equation for estimating Fe^{3+} concentrations in ferromagnesian silicates and oxides from microprobe analyses, using stoichiometric criteria. *Mineral. Mag.*, **51:** 431-435.

EDGAR, A. D., (1984), Chemistry, occurrence and paragenesis of feldspathoids. A review. *In*: BROWN, W. L. (ed.) – *Feldspars and feldspathoids*. D. Reidel Publishing Company, p. 501-532.

FREITAS, R. O., (1947), Geologia e petrologia da Ilha de São Sebastião. *Bol. Fac. Fil. Ciênc. Letr. USP*, **85:** 1-244. (*Geologia* **3**)

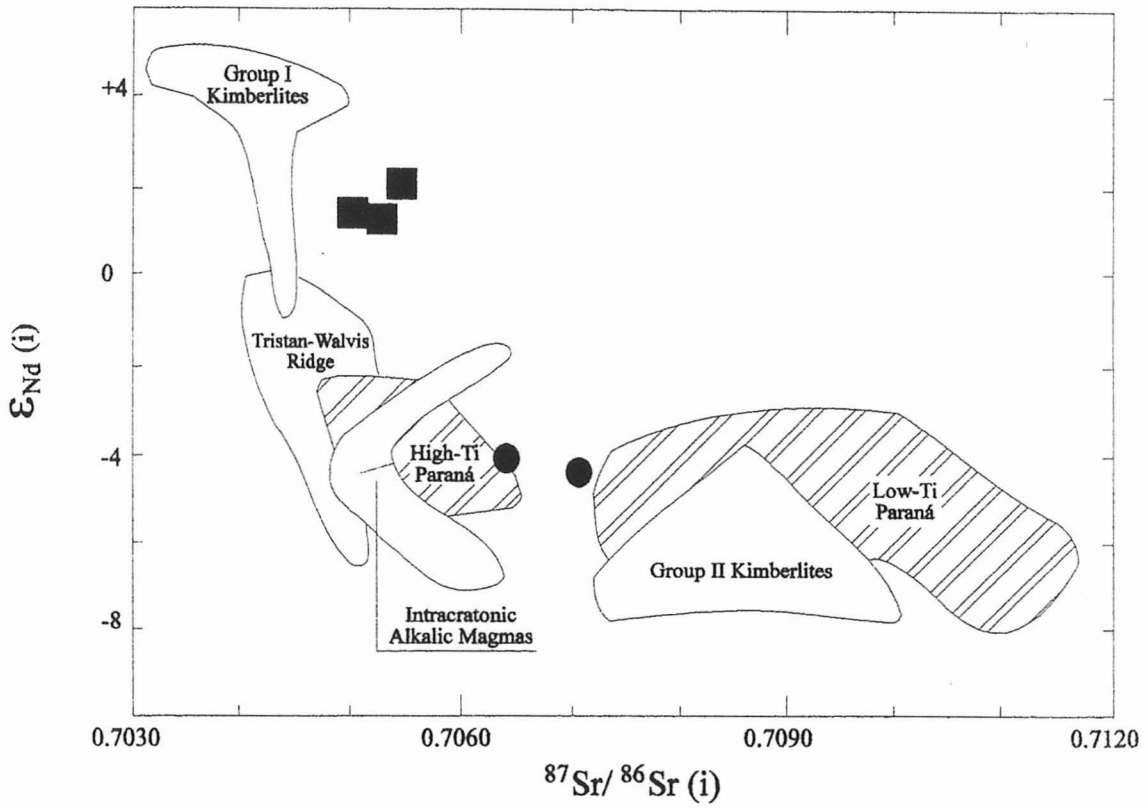

Fig. 7 — Nd and Sr isotopic compositions (Tab. V) in comparison to Intracratonic Alkalic Magmas (Carlson *et al.*, 1993), Paraná basalts, South African kimberlites and Ocean Island Basalts (OIB, Tristan-Walvis Ridge hot spot). ● = BAS; ■ = LAMP.

FREITAS, R. O., (1976), Definição petrológica, estrutural e geotectônica das cintas orogênicas antigas do litoral norte do Estado de São Paulo. *Bol. Inst. Geol.,* **1:** 1-176.

GARDA, G. M., (1995), *Os diques básicos e ultrabásicos da região costeira entre as cidades de São Sebastião e Ubatuba, Estado de São Paulo.* 360p. (PhD thesis submitted to the Instituto de Geociências, Universidade de São Paulo).

GARDA, G. M.; JULIANI, C.; SCHORSCHER, J. H. D.; NEUMANN, R. & BOHLAND NETO, F., (1992), Vulcanismo recorrente e feições geológicas afins em diques básicos-ultrabásicos da Praia Vermelha do Sul, Município de Ubatuba/SP. *In*: Jornadas Científicas do Instituto de Geociências da USP, 2, São Paulo, 1992. Bol. IG-USP. *Publicação Especial,* **12:** 45-46.

GOMES, C. B., (1973), Comportamento dos feldspatos do dique de diabásio de Toninhas, Ubatuba. *In*: Congresso Brasileiro de Geologia, 27, Aracaju, 1973. Aracaju, SBG. *Boletim,* **1:** 75.

GOMES, C. B., (1974), Mineralogia do dique de Toninhas, Ubatuba, litoral norte do Estado de São Paulo: Feldspatos. *Rev. Bras. Geoc.,* **4:** 80-87.

GOMES, C. B. & RUBERTI, E., (1979), Mineralogia do dique de Toninhas, Ubatuba, litoral norte do Estado de São Paulo: Piroxênios. *Bol. Miner.,* **6:** 55-66.

GOMES, C. B. & BERENHOLC, M., (1980), Some geochemical features of the Toninhas dyke, Ubatuba, State of São Paulo, Brazil. *An. Acad. bras. Ci.,* **52:** 339-346.

HART, (1984), A large-scale isotope anomaly in the Southern Hemisphere mantle. *Nature,* **309:** 753-757.

LEAKE, B. E., (1978), Nomenclature of amphiboles. *Can. Mineral.,* **16:** 501-520.

MINIOLI, B., (1969), *Determinações K-Ar em rochas localizadas próximas ou no litoral norte do Estado de São Paulo.* 19p. (MSc Dissertation. Instituto de Geociências, Universidade de São Paulo).

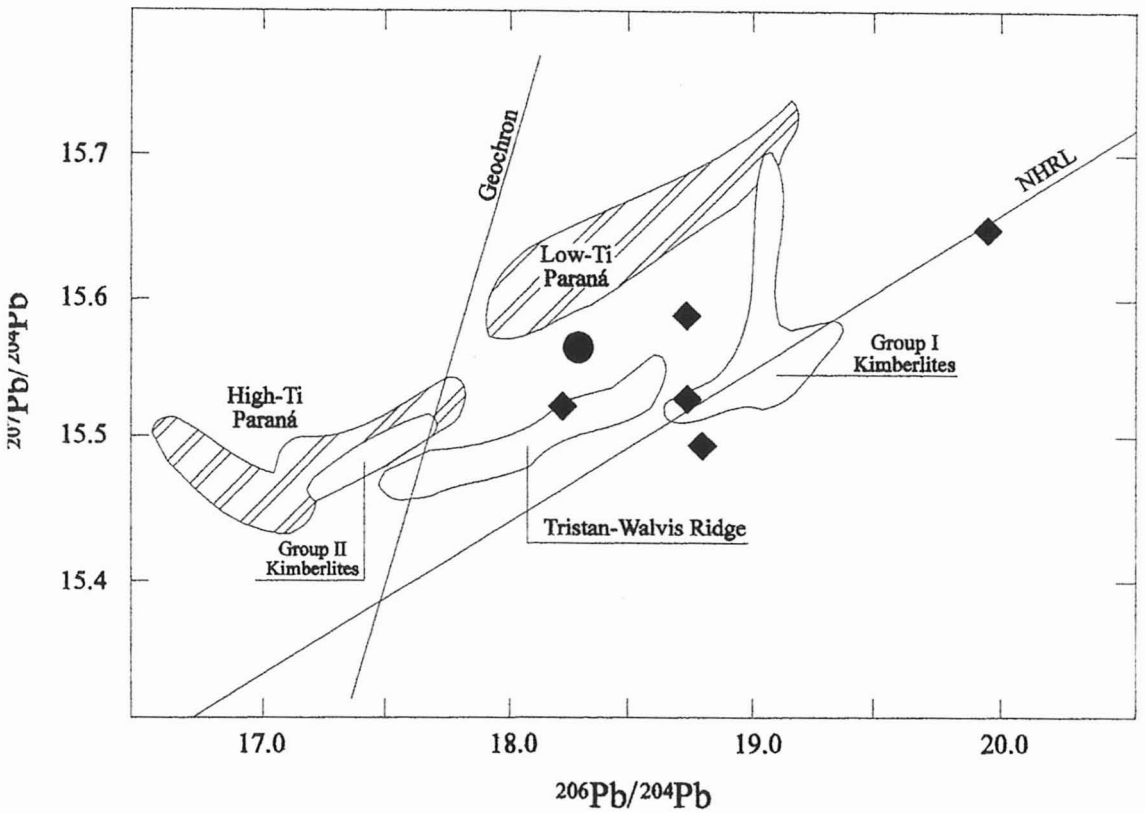

Fig. 8 — Pb isotopic compositions (Tab. V) in comparison to Paraná basalts, South African kimberlites and OIB (Tristan-Walvis Ridge hot spot). The alnöite sample PCa-1 is the most Pb radiogenic. ● = BAS; ◆ = LAMP.

MINIOLI, B.; PONÇANO, W. L. & OLIVEIRA, S. M. B. DE, (1971), Extensão geográfica do vulcanismo basáltico do Brasil meridional. *An. Acad. bras. Ci.*, **43** (2): 433-437.

MONTES-LAUAR, C. R.; PACCA, I. G.; MELFI, A. J.; PICCIRILLO, E. M.; BELLIENI, G. & DEMIN, A., (1990), Mesozoic dyke swarm of the São Sebastião Island (SE Brazil): Paleomagnetism and geochemistry. *In*: International Dyke Conference, 2, Adelaide, Australia, 1990. *Abstracts*.

MORIMOTO, N., (1988), Nomenclature of pyroxenes. *Am. Mineral.*, **73:** 1123-1133.

PICCIRILLO, E. M.; COMIN-CHIARAMONTI, P.; MELFI, A. J.; STOLFA, D.; BELLIENI, G.; MARQUES, L. S.; GIARETTA, A.; NARDY, A. J. R.; PINESE, J. P. P.; RAPOSO, M. I. B. & ROISENBERG, A., (1988a), Petrochemistry of continental flood basalt-rhyolite suites and related intrusives from the Paraná Basin (Brazil). *In*: PICCIRILLO, E. M. & MELFI, A. J. (eds.) – *The Mesozoic flood volcanism of the Paraná Basin*. São Paulo, IAG-USP, p. 107-156.

PICCIRILLO, E. M.; MELFI, A. J.; COMIN-CHIARAMONTI, P.; BELLIENI, G.; ERNESTO, M.; MARQUES, L. S.; NARDY, A. J. R.; PACCA, I. G.; ROISENBERG, A. & STOLFA, D., (1988b), Continental flood volcanism from the Paraná Basin (Brazil). *In*: MACDOUGALL, J. D. (ed.) – *Continental flood basalts*. Dordrecht, Klumer Academic Publishers, 341p.

ROCK, N. M. S., (1979), Petrology and origin of the type monchiquites and associated lamprophyre dykes of Serra de Monchique, Portugal. *Trans. R. Soc. Edinburgh*, **70:** 149-170.

ROCK, N. M. S., (1986), The nature and origin of ultramafic lamprophyres: Alnöites and allied rocks. *J. Petrol.*, **27:** 155-196.

ROCK, N. M. S., (1991), *Lamprophyres*. Blackie & Son Ltd., 285p.

SILVA, A. T. S. F.; CHIODI FILHO, C.; CHIODI, D. K. & PINTO FILHO, W. D., (1977), Convênio DNPM-CPRM – *Projeto Santos-Iguape*. Vol. 1: Geologia, 639p.

SONOKI, I. K. & GARDA, G. M., (1988), Idades K-Ar de rochas alcalinas do Brasil Meridional e Paraguai Oriental: Compilação e adaptação às novas constantes de decaimento. *Bol. IG-USP, Série Científica,* **19:** 63-85.

STEIGER, R. H. & JAEGER, E., (1977), Subcommission on Geochronology: convention on the use of decay constants in Geochronology and Cosmochronology. Contribution to the Geologic Time Scale. AAPG. *Studies in Geology,* **6:** 67-71.

SUN, S-S. & MCDONOUGH, W. F., (1989), Chemical and isotopic systematics of ocean basalts: implications for mantle composition and processes. *In*: SAUNDERS, A. D. & NORRY, M. J. (eds.) – *Magmatism in the ocean basins.* Geological Society Special Publication, **42:** 313-345.

ULBRICH, H. H. G. J. & GOMES, C. B., (1981), Alkaline rocks from continental Brazil. *Earth-Sci. Rev.,* **17:** 135-154.

ULBRICH, H. H. G. J.; GARDA, G. M. & ULBRICH, M. N. C., (1991), Avaliação das idades K/Ar dos maciços alcalinos do Brasil Sul-Oriental e Paraguai Oriental. *Bol. IG-USP, Publicação Especial,* **9:** 87-92.